

## RESEARCH ARTICLE

# Strong positive allometry of bite force in leaf-cutter ants increases the range of cuttable plant tissues

Frederik Püffel<sup>1,\*</sup>, Flavio Roces<sup>2</sup> and David Labonte<sup>1,\*</sup>

## ABSTRACT

*Atta* leaf-cutter ants are the prime herbivore in the Neotropics: differently sized foragers harvest plant material to grow a fungus as a crop. Efficient foraging involves complex interactions between worker size, task preferences and plant–fungus suitability; it is, however, ultimately constrained by the ability of differently sized workers to generate forces large enough to cut vegetation. In order to quantify this ability, we measured bite forces of *Atta vollenweideri* leaf-cutter ants spanning more than one order of magnitude in body mass. Maximum bite force scaled almost in direct proportion to mass; the largest workers generated peak bite forces 2.5 times higher than expected from isometry. This remarkable positive allometry can be explained via a biomechanical model that links bite forces with substantial size-specific changes in the morphology of the musculoskeletal bite apparatus. In addition to these morphological changes, we show that bite forces of smaller ants peak at larger mandibular opening angles, suggesting a size-dependent physiological adaptation, probably reflecting the need to cut leaves with a thickness that corresponds to a larger fraction of the maximum possible gape. Via direct comparison of maximum bite forces with leaf mechanical properties, we demonstrate (i) that bite forces in leaf-cutter ants need to be exceptionally large compared with body mass to enable them to cut leaves; and (ii), that the positive allometry enables colonies to forage on a wider range of plant species without the need for extreme investment in even larger workers. Our results thus provide strong quantitative arguments for the adaptive value of a positively allometric bite force.

**KEY WORDS:** Allometric scaling, Biomechanics, Foraging, Insects

## INTRODUCTION

Leaf-cutter ants are remarkable in many ways. They are the world's first farmers; their colonies collect plant material to grow a fungus as a crop – a mutualism that originated around 50 million years ago (Mueller et al., 2001; Hölldobler and Wilson, 2010). They are considered the principal herbivore in the Neotropics; *Atta* ants are estimated to consume about 15% of the foliar biomass produced by Neotropical trees (Fowler et al., 1989; Costa et al., 2008). And last,

they display a level of polymorphism, linked to size-dependent task preferences and a complex ecology, exceptional even within social insects (e.g. Wilson, 1980a; Wirth et al., 2003).

Among the diverse tasks arising in a leaf-cutter ant colony are brood care, fungus gardening, worker transport, soil excavation, nest defence and foraging (Wilson, 1980a; Hölldobler and Wilson, 2010; Pielström and Roces, 2013). In particular, foraging behaviour has received considerable attention, as it is central to leaf-cutter ant ecology (e.g. Wilson, 1980a,b, 1983a,b; Rudolph and Loudon, 1986; Wetterer, 1990; Roces, 1990; Roces and Núñez, 1993; Roces and Hölldobler, 1994; Wetterer, 1994a,b, 1995a,b; Burd, 1995, 1996, 2000a,b, 2001; Roces and Hölldobler, 1996; Farji-Brener, 2001; Röschard and Roces, 2002, 2003, 2011; Farji-Brener and Sasal, 2003; Burd and Howard, 2005; Dussutour et al., 2008; Moll et al., 2010, 2013). Key to foraging success is the cutting of small fragments from vegetation – the energetically most demanding task faced by the colony (Roces and Lighton, 1995). Although many aspects of foraging involve complex biological interactions (e.g. Roces, 2002), cutting plant fragments is, at its core, a mechanical problem: the ability to cut a leaf or fruit is determined by the maximum available bite force, the morphology of the mandible, and the material and structural properties of the plant. Perhaps surprisingly, this mechanical foundation of leaf-cutting has received comparatively little quantitative attention (e.g. Tautz et al., 1995; Schofield et al., 2011, 2016). Larger workers possess larger mandible closer muscles and may thus be reasonably expected to produce larger bite forces, which may in turn enable them to cut a wider range of plant materials. Indeed, they tend to be more likely to cut tougher and denser leaves (Cherrett, 1972; Wilson, 1980a,b; Nichols-Orians and Schultz, 1989, 1990; Wetterer, 1991). Understanding the exact relationship between bite force and worker size is crucial for the analysis of leaf-cutter ant foraging behaviour, because it holds the key to distinguish between foraging assignments based on ability (which ants can cut a given leaf) versus suitability (which ants should cut a given leaf). This distinction is relevant for assessing the evolution and possible adaptive advantage of worker polymorphism, and for predictions on 'optimal' foraging strategies based on ergonomic considerations (e.g. Wilson, 1980b; Wetterer, 1991; Burd and Howard, 2005).

We previously predicted the scaling of bite force based on the morphology of the bite apparatus in *Atta vollenweideri* leaf-cutter ants (Püffel et al., 2021). However, direct experimental confirmation of this prediction is missing and difficult to obtain, because ants are small. To make matters worse, bite forces in insects generally depend on the mandibular opening angle (Goyens et al., 2014; Weihmann et al., 2015a; Püffel et al., 2023), which is challenging to control experimentally. Here, we addressed both difficulties with the help of a custom-built bite force set-up and first principles biomechanical analysis. We report direct bite force measurements for ant workers spanning more than one order of

<sup>1</sup>Department of Bioengineering, Imperial College London, London, SW7 2AZ, UK.  
<sup>2</sup>Department of Behavioural Physiology and Sociobiology, University of Würzburg, 97074 Würzburg, Germany.

\*Authors for correspondence (f.puffel18@imperial.ac.uk; d.labonte@imperial.ac.uk)

© F.P., 0000-0002-3917-0942; F.R., 0000-0001-9258-3079; D.L., 0000-0002-1952-8732

This is an Open Access article distributed under the terms of the Creative Commons Attribution License (<https://creativecommons.org/licenses/by/4.0>), which permits unrestricted use, distribution and reproduction in any medium provided that the original work is properly attributed.

### List of symbols and abbreviations

$A_{\text{phys}}$	physiological cross-sectional area of the mandible closer muscle
$\hat{e}_1, \hat{e}_2, \hat{e}_3$	local head coordinate system
$F_b$	applied bite force
$F_{b,m}$	measured bite force
$F_{b,\text{max}}$	maximum bite force at an equivalent mandibular opening angle, $\theta_{\text{max}}$
$F_{b,\theta}$	maximum bite force at opening angle $\theta$
$F^*$	bite force–opening angle relationship, normalised with its maximum
$F_{\theta}^*$	relative bite force at opening angle $\theta$
$L_f$	average muscle fibre length
$L_{i,\text{eff}}$	effective mandible in-lever
$L_{o,c}$	mandible out-lever at bite contact point
$L_{o,\text{eff},c}$	effective mandible out-lever at bite contact point
$L_{o,d}$	most distal (largest) mandible out-lever
$L_{o,\text{eff},d}$	most distal (largest) effective mandible out-lever
$L_{\text{opt}}$	optimal muscle fibre length at which muscle stress is maximal
$L_p$	lever arm length around the beam pivot during biting experiment
$L_{p,\text{cal}}$	lever arm length around the beam pivot during sensor calibration
$R$	rotational axis of the mandible joint
$S_l$	vector connecting joint centre with left head spike
$S_r$	vector connecting joint centre with right head spike
$\alpha$	misalignment angle between $F_{b,m}$ and $F_b$
$\beta$	muscle force–length shape parameter
$\Gamma$	correction term for differences in lever arm around the beam pivot (correction 2)
$\theta$	mandibular opening angle
$\theta_{\text{max}}$	mandibular opening angle at which bite force is maximal
$\theta_{\text{opt}}$	mandibular opening angle at which muscle stress is maximal
$\sigma$	muscle stress
$\sigma_{\text{max}}$	maximum muscle stress
$\phi$	average fibre pennation angle

magnitude in body mass, relate our results to the foraging behaviour of leaf-cutter ant colonies, and discuss both the magnitude and scaling of bite forces in a comparative framework.

## MATERIALS AND METHODS

### Study animals

Bite force experiments were conducted with *Atta vollenweideri* Forel 1893 ants from three colonies, all founded and collected in Uruguay in 2014 (see Fig. 1A). The colonies were kept at 25°C and 50% humidity in a climate chamber under a light:dark cycle of 12 h:12 h, and were fed with fresh bramble leaves, cornflakes and honey water *ad libitum*. We collected around 80 workers from the foraging areas of each colony ( $n=248$ ), covering approximately the entire size range (1–50 mg). We excluded minims (body mass <1 mg), because their bite apparatus is morphologically distinct (N. Imirzian, F.P., F.R. and D.L., unpublished), and they do not generally partake in foraging (Wilson, 1980a).

### Experimental set-up

Bite forces were measured with a custom-built set-up based on a capacitive force sensor (SingleTact S8-1N, Pressure Profile Systems, Inc., Los Angeles, CA, USA; data acquisition frequency 33 Hz, maximum force 1 N, resolution 2 mN). In order to distribute the force equally across the sensor area, we used a lever mechanism to convert point-like bite forces into an areal compression (see Fig. 1B). Ants bit onto two thin bite plates (1 mm long, and ~0.15 mm thick; see Fig. 1D), protruding from two mechanically uncoupled beams (6×6×40 mm and 6×12×6 mm, respectively).

Both beams and the terminating bite plates were manufactured in one single piece from stainless steel to minimise compliance, using electrical discharge machining. The beam that transmits the bite force to the sensor (the pivoting beam) was connected to a metal base plate, made from a single aluminium block using CNC milling, via a small hinge placed in the beam centre. As an ant bites onto the bite plates, the opposite end of this pivoting beam is pressed onto the sensor, which is glued to a vertical wall protruding from the base. At the maximum load of 1 N, the sensor only deforms approximately 10  $\mu\text{m}$  (manufacturer's data). Because the gear ratio of the pivoting beam is unity, the magnitude of this deformation is equivalent to the maximum displacement of the bite plate arising from beam rotation. As bite plate bending is also negligible (see Supplementary Materials and Methods), we measured approximately isometric bite forces. The second beam (the sliding beam), in turn, was connected to a lubricated rail, so that its position relative to the pivoting beam could be altered via a stepper motor (28BYJ-48, 5 V) connected to a gearing system 3D printed from PLA. This design allowed us to vary the distance between the two bite plates by less than 100  $\mu\text{m}$  per motor step. The minimum required gap to bite both bite plates, equivalent to the shortest distance between their outer surfaces, was 0.5 mm, and the largest gap used during experiments was 3.0 mm. This range is similar to the range of head widths of the ants used in this experiment (1.1–4.5 mm).

In order to extract coordinates of key landmarks (see below), a top-down camera was synchronised to the sensor recording, and recorded the bite experiments at 30 frames  $\text{s}^{-1}$  (camera module v. 2.1, 8 MP, Raspberry Pi Foundation, Cambridge, UK; with a Black Eye HD macro lens, Eye Caramba Ltd, Helsinki, Finland). A mirror, tilted 45 deg with respect to the camera plane, provided depth information. A force sensor, motor, camera and a touchscreen (7 inch HDMI-LCD Display, Elecrow, Shenzhen, China) were connected to a Raspberry Pi (v. 3B+, Raspberry Pi Foundation). The system was operated via custom software written in Python v. 3.5 (see Supplementary Materials and Methods for details on the user interface and circuit; see also Van Rossum and Drake, 2009).

### Sensor calibration, accuracy and precision

The sensor was calibrated using a series of calibration weights (Kern & Sohn GmbH, Balingen, Germany), suspended from the pivoting lever via a thin cotton thread (the mass of the cotton thread was small, ~0.015 g, and hence neglected). The thread was placed at around one-quarter of the length of the bite plate measured from its base, resulting in a moment arm around the pivot of  $L_{p,\text{cal}} \approx 20.25$  mm. The set-up was rotated such that the measurable force vector aligned with gravity (see Fig. 1E). We used 20 masses between 5 and 100 g; a mass of 1.4 g was required to establish equilibrium around the pivot, and was consequently subtracted from all readings. The range of effective weight forces was hence 35–970 mN, approximately spanning the range of measured bite forces. Each weight was suspended 5 times in random order, and the steady-state sensor reading averaged across ~2 s was used for sensor calibration. The relationship between weight and sensor output was characterised via an ordinary least squares regression on  $\log_{10}$ -transformed data in order to prioritise minimisation of relative error over absolute error; the high  $R^2$  of the regression line indicates robust calibration ( $R^2=0.993$ ; see Fig. 1E).

To quantify calibration accuracy and precision, five additional masses (7–87 g) were measured 3 times each, and the relative error was calculated as  $\epsilon=1-|F_w|/|F_x|$ , where  $F_x$  is the predicted and  $F_w$  is the measured force, respectively (see Fig. 1F). Throughout

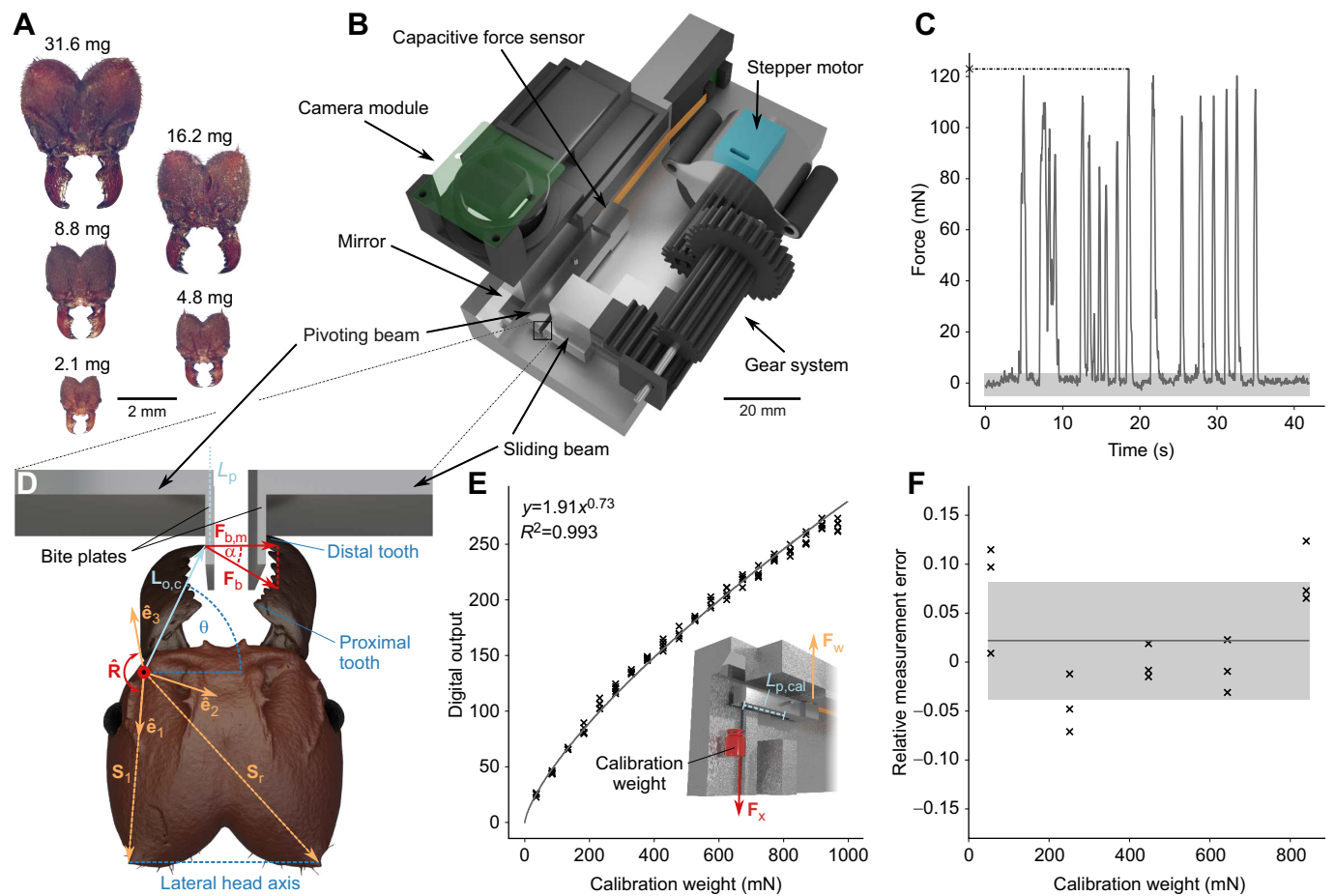


**Fig. 1. Experimental set-up.** (A) We measured bite forces of polymorphic *Atta vollenweideri* leaf-cutter ants ranging between 1.5 and 46.8 mg in body mass. (B) To measure bite forces, we built a custom-designed force set-up based on a capacitive force sensor and a lever mechanism. The ants bit onto two bite plates, one protruding from a pivoting beam connected to the force sensor, the other protruding from a sliding beam. The distance between the two bite plates could be varied by moving the sliding beam via a geared stepper motor. Bite experiments were filmed with a top-down camera, which also recorded a side view from a 45 deg mirror. (C) When placed in front of the bite plates, ants readily bit. The measured forces exceeded the sensor noise (shaded area) by at least a factor of eight. From each force trace, the maximum force (cross) was extracted for further analysis. (D) From the video recordings, we further extracted the coordinates of the mandible joint centre, head spikes  $S_1$  and  $S_2$ , bite contact point with a distance  $L_p$  to the beam pivot, mandible out-lever length  $L_{o,c}$ , and the most distal and proximal tooth tips (for more details, see Supplementary Materials and Methods). The rotational axis of the mandible  $\hat{R}$  was projected onto the local head coordinate system ( $\hat{e}_1, \hat{e}_2, \hat{e}_3$ ). The mandibular opening angle  $\theta$  was defined as the angle between the lateral head axis, spanned by the head spikes, and the projection of the largest out-lever onto the plane of rotation. The magnitude of the bite force  $|F_b|$  was extracted from the measured force  $|F_{b,m}|$  and the misalignment angle  $\alpha$ , extracted from the video recordings, as defined by Eqn 1. For simplicity, the depicted ant bites with its largest out-lever, i.e. with the tip of the most distal tooth  $L_{o,c} = L_{o,d}$ , and all vectors are shown in the plane of rotation, i.e. they indicate the effective out-lever,  $L_{o,eff}$  (for more details, see Supplementary Materials and Methods). The head orientation during experiments, however, may be different; angles  $\theta$  and  $\alpha$  were thus not measured directly from the recordings, but were inferred indirectly via their vector-algebraic basis, using  $\hat{R}$  and the local coordinate system ( $\hat{e}_1, \hat{e}_2, \hat{e}_3$ ; see Materials and Methods). (E) For sensor calibration, masses between 5 and 100 g were suspended from the bite plate of the pivoting lever at a distance  $L_{p,cal}$  to the pivot. A linear regression on  $\log_{10}$ -transformed data characterised the relationship between measured output and force with high accuracy ( $R^2=0.993$ ). (F) A subsequent error analysis using intermediate masses between 7 and 87 g yielded a mean relative error of 2% (accuracy, black line) with a standard deviation of 6% (precision, shaded area), independent of weight (see Materials and Methods).

this text, we write vectors as bold; unit vectors are labelled with a hat (as in  $\hat{R}$ ). The average measurement error, the sensor accuracy, was  $2 \pm 6\%$  independent of weight [linear mixed model (LMM) with weight as fixed and repetition as random effect:  $\chi^2_1=0.38, P=0.53$ ; the average magnitude of the measurement error was  $5 \pm 4\%$ ]; the standard deviation indicates the precision of the measurements.

To quantify sensor noise, the output of the unloaded sensor was recorded for 100 s. Discrete Fourier transformation suggested a constant power spectral density, indicating white noise (Haykin, 2001, p. 61). This noise had a standard deviation of 1 mN and a range of  $-5$  to 4 mN. The maximum positive value of this range was

about 8 times smaller than the smallest measured bite force (see Fig. 1C). Sensor drift was significant (Spearman's correlation coefficient:  $r_{S,2867} = -0.26, P < 0.001$ ; see manufacturer's data sheet), but small enough to be inconsequential across the time scale of our measurements (cf.  $1 \text{ mN min}^{-1}$  versus  $\sim 30\text{--}60 \text{ s}$ ).

In a last validation step, we directly compared measurements with our set-up with those of an established set-up based on a substantially more expensive piezoelectric sensor (Herrel et al., 1999; Rühr and Blanke, 2022). To this end, maximum bite forces of three house crickets (*Acheta domesticus*) were measured with three repetitions on both set-ups, by two independent operators each. A LMM with set-up and operator as fixed effect and specimen



as random effect showed no significant influence of either set-up or operator on bite force (LMM versus random intercept model:  $\chi^2_2=3.83$   $P=0.15$ ; set-up:  $t_{31}=1.68$ ,  $P=0.10$ ; operator:  $t_{31}=0.95$ ,  $P=0.35$ ).

The camera was calibrated assuming an inverse size–distance relationship,  $L_2S_2=L_1S_1$ , where  $S_1$  and  $S_2$  are the apparent sizes of an object at distances  $L_1$  and  $L_2$  to the camera aperture. The apparent size of a calibration target (5 units on 1 mm-grid paper), placed on the top surface of the metal base at a distance  $L_1\approx 32$  mm to the camera, was measured from 10 images, and the pixel-to-mm conversion factor  $C_1$  was extracted. This conversion factor changes approximately in direct proportion to the camera distance as  $C_2=C_1L_2/L_1$ , where  $L_2$  is the distance between the camera and the imaged object. In contrast to  $L_1$ ,  $L_2$  is not constant, but varies with the vertical position of the object coordinate, which was extracted using the mirrored side view.

For validation, the grid paper was photographed at 25 different positions along the bite plate, extracted from five trials, and its physical size was calculated from the calibration. The relative error was  $1\pm 2\%$ . This error changed significantly with grid paper–lens distance – the physical dimensions were increasingly underestimated at smaller distances (LMM with lens distance as fixed effect and trial as random effect:  $\chi^2_1=6.94$ ,  $P<0.01$ ). This effect, however, was miniscule (1.5% across the entire bite plate length, 6 mm), corresponding to only  $\sim 60$   $\mu\text{m}$ , or about 10% of the smallest measured mandible length; it is thus considered negligible.

### Experimental protocol

To measure bite forces, individual ants were held in front of the bite plates using insect tweezers. Ants were eager to bite, typically executing numerous bite cycles in quick succession (see Fig. 1C). After completing at least five bite cycles, or exceeding a total bite duration of 10 s, the measurement was terminated, each ant was weighed (AX304 Microbalance, maximum capacity 310 g, readability 0.1 mg, Mettler Toledo, Greifensee, Switzerland) and isolated, and the maximum force was extracted. To obtain bite forces from a maximum range of sizes and varying opening angles without pseudoreplication, we measured each ant only once at a single bite plate distance. In practice, we gradually increased the bite plate distance from 0.5 to 3.0 mm; for each distance, we used ants of all sizes capable of biting onto the plates. For small plate distances, this included almost all ants; for the largest plate distance, however, only larger specimens were able to bite. We assume that ants bit with maximum muscle activation at all opening angles, as indicated by measurements involving direct muscle stimulation in the closely related *Atta cephalotes* (Püffel et al., 2023).

### Extraction of landmarks

In order to obtain the opening angle, the orientation of the bite force vector and the length of the mandible out-lever (see below), we extracted the coordinates of a series of landmarks from the video frame corresponding to the time of maximum bite: (i) the contact point between the mandible and bite plate; (ii) the tip of the most distal and proximal mandibular teeth; (iii) the mandible joint centre (defined as in Püffel et al., 2021); and (iv) a pair of distinct head spikes (see Fig. 1D; Fig. S1). In addition, we extracted the orientation of the mandible joint axis  $\hat{\mathbf{R}}$  via kinematics analysis of the mandible motion (Püffel et al., 2023; V. Kang, F.P. and D.L., unpublished). In order to position  $\hat{\mathbf{R}}$  on the biting ant, we introduced a local head coordinate system ( $\hat{\mathbf{e}}_1$ ,  $\hat{\mathbf{e}}_2$ ,  $\hat{\mathbf{e}}_3$ ) based on the vectors connecting the joint centre with the tips of both head spikes,  $\mathbf{S}_1$  and  $\mathbf{S}_2$ , respectively. The coordinate axes were defined as  $\hat{\mathbf{e}}_1=\mathbf{S}_1/|\mathbf{S}_1|$ ,

$\hat{\mathbf{e}}_3=(\mathbf{S}_1\times\mathbf{S}_2)/|\mathbf{S}_1\times\mathbf{S}_2|$  and  $\hat{\mathbf{e}}_2=\hat{\mathbf{e}}_3\times\hat{\mathbf{e}}_1$ . The estimated rotational axis was then projected onto this local head coordinate system (for more details, see Supplementary Materials and Methods). In line with previous work (Weihmann et al., 2015b), we define the opening angle as the angle between the lateral head axis and the largest effective out-lever. The lateral head axis was defined as the vector connecting both head spikes ( $\mathbf{S}_1-\mathbf{S}_2$ ; see Fig. 1D); the largest effective out-lever was defined as the length of the vector which connects the tip of the most distal mandible tooth and the joint rotational axis in the plane of rotation,  $\mathbf{L}_{o,\text{eff},d}=\mathbf{L}_{o,d}-(\hat{\mathbf{R}}\cdot\mathbf{L}_{o,d})\hat{\mathbf{R}}$ , where  $\mathbf{L}_{o,d}$  is any vector which connects the most distal tooth tip and the rotational axis (see Supplementary Materials and Methods for more details). The opening angle then follows from basic vector algebra as  $\theta=\arccos[\mathbf{L}_{o,\text{eff},d}\cdot(\mathbf{S}_1-\mathbf{S}_2)/(|\mathbf{L}_{o,\text{eff},d}||\mathbf{S}_1-\mathbf{S}_2|)]$ .

### Confounding effects due to size differences

Measuring bite forces across a large size range poses at least two challenges. First, the signal-to-noise ratio typically decreases with animal size, as smaller animals generally bite with less force. We addressed this challenge by selecting a force sensor capable of measuring small and large bite forces with sufficiently high resolution (see above). Second, the characteristic dimensions of the set-up are relatively larger for small animals. The implications of this size effect are perhaps less obvious and, unfortunately, more complex. To appreciate the problem, consider a small ant of 3 mg body mass biting onto bite plates that are 1 mm apart. This bite plate distance is approximately equal to the distance between the two mandible joints; a bite with the distal-most teeth would thus involve a mandibular opening angle of about 90 deg. For a bite with the most proximal teeth, in turn, the opening angle is larger, around 110 deg (see Fig. 1A), and the effective out-lever is smaller. Consider next a large ant of 45 mg biting onto the same bite plates. For a distal bite, the bite plate distance corresponds to only 40% of the joint distance, and thus a much lower opening angle of about 70 deg. Notably, the ant's ability to bite with proximal parts of her mandible is limited because the length of the mandible blade exceeds the length of the bite plate by about 20% (see Fig. 1D). Evidently, for a given configuration of the experimental set-up, both the range of possible mandibular opening angles and bite positions along the mandible blade vary systematically with size. Because both directly affect the magnitude of bite force (see Eqn 3, below; Püffel et al., 2023), an unbiased comparison of bite force magnitude across animal sizes requires four corrective steps, implemented here with the ultimate aim to extract the maximum bite force an ant worker can produce when biting with an equivalent point of her mandible (the tip of the most distal mandible tooth; see Fig. 2). First, we correct for the misalignment between measurable force vector,  $\mathbf{F}_{b,m}$ , and applied bite force vector,  $\mathbf{F}_b$ . Second, we correct for differences in moment arms around the bite lever pivot, arising from variation of the mandible contact point along the bite plate. Third, we account for variation in bite position along the mandible blade, which alters the mechanical advantage of the force transmission system. Fourth, we account for differences in mandibular opening angle.

The first correction is necessary because the sensor measures 1D compression,  $\mathbf{F}_{b,m}$ , but the applied bite force vector,  $\mathbf{F}_b$ , may deviate from this line of action by a misalignment angle  $\alpha$  (see Fig. 1D). The orientation of  $\mathbf{F}_{b,m}$  is approximately equal to the plane normal of the bite plate; the orientation of the bite force vector is defined by the cross-product between the mandible out-lever  $\mathbf{L}_{o,c}$  and the rotational axis, where  $\mathbf{L}_{o,c}$  is any vector connecting the joint axis of rotation and the bite contact point (for more details, see Püffel et al., 2023). The resulting correction factor reads

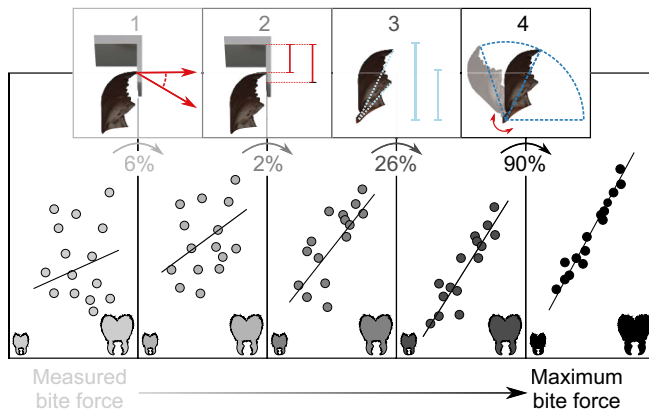


**Fig. 2. Applied corrections to measured forces.** In order to extract the maximum bite force from the measured data, we account for four confounding effects: (1) the misalignment between bite force orientation and the force-sensitive axis; (2) variation in bite contact point on the bite plate, which results in different moment arms; (3) differences in bite position along the mandible blade, which determines the mechanical advantage of the musculoskeletal force transmission system; and (4) variation in mandibular opening angle, which is associated with variation in mechanical advantage, fibre length and pennation angle, all of which influence bite force. Implementation of these corrections reduces the size-dependent variation introduced by the experimental design and animal behaviour, and thus enables an unbiased comparison of maximum bite force capacity across animals of different sizes. The data depicted in this schematic diagram are not 'real' data, but merely serve for illustration. The 'actual' relative change in force caused by each correction, averaged for all ants, is shown as a percentage.

$1/\cos\alpha = (|\mathbf{L}_{o,c} \times \hat{\mathbf{R}}| \cdot |\mathbf{F}_{b,m}|) / ((\mathbf{L}_{o,c} \times \hat{\mathbf{R}}) \cdot \mathbf{F}_{b,m})$  (for more details, see Püffel et al., 2023). This correction was typically larger for larger animals, which more frequently bit at opening angles below 90 deg (see Results), leading to larger misalignment angles.

The second correction is necessary because the point of force application on the bite plate itself may vary across ants – smaller ants have shorter mandibles and are thus more likely to bite at the distal end part of the bite plates (see Fig. 1D). For each bite, we thus measured the lever arm around the bite lever pivot,  $L_p$ , defined as the distance between the bite contact point and the pivot in the plane of rotation. To remove variation due to  $L_p$ , we introduce the correction term  $\Gamma = L_{p,cal}/L_p$ , where  $L_{p,cal}$  is the distance between the pivot and the point of application of weights during sensor calibration.  $\Gamma$  was always close to 1, as the length of the bite plate is small in comparison to  $L_{p,cal}$  (~5%); the effect of this correction was thus miniscule.

The third correction is necessary because the bite force may be transferred onto the bite plate at an arbitrary position along the mandible; an ant biting with the distal end of its mandible may use the same muscle effort but nevertheless produce a smaller measured bite force than an ant biting with the proximal end of its mandible, because the mechanical advantage of the force transmission system differs (e.g. Lappin and Jones, 2014). To correct for this variation, we converted the measured bite force into an equivalent bite force at a fixed point on the mandible blade (the most distal tooth tip). To this end, we extracted the length of the vector which connects the contact point between the mandible and bite plate with the joint rotational axis in the plane of rotation,  $\mathbf{L}_{o,eff,c}$  – the effective out-lever of the bite force measurement. We then calculated the bite force for a hypothetical bite exerted via the tip of the most distal tooth, characterised by an effective out-lever  $\mathbf{L}_{o,eff,d}$  (see above and Püffel et al., 2023, for more details).

After implementation of corrections i–iii, the magnitude of the bite force  $|\mathbf{F}_{b,\theta}|$  follows as:

$$|\mathbf{F}_{b,\theta}| = \Gamma \frac{|\mathbf{F}_{b,m}| |\mathbf{L}_{o,eff,c}|}{\cos \alpha |\mathbf{L}_{o,eff,d}|}. \quad (1)$$

A fourth and last correction is then necessary, because bite forces vary systematically with mandibular opening angle (Dumont and Herrel, 2003; Gidmark et al., 2013; Goyens et al., 2015; Weihmann et al., 2015a; Kaczmarek and Gidmark, 2020; Püffel et al., 2023). In general, the bite force at any opening angle may be written as the product between muscle stress  $\sigma$ , the physiological cross-sectional area of the mandible closer muscle  $A_{phys}$ , the average pennation angle  $\phi$  of the muscle fibres, and the mechanical advantage of the mandible lever system, defined as the ratio between the effective in-lever and out-lever  $|\mathbf{L}_{i,eff}|/|\mathbf{L}_{o,eff}|$  (see Püffel et al., 2021, 2023, for details):

$$|\mathbf{F}_b| = \sigma A_{phys} \cos \phi \frac{|\mathbf{L}_{i,eff}|}{|\mathbf{L}_{o,eff}|}. \quad (2)$$

Here, the effective in-lever is the length of the shortest vector which connects the line of action of the net muscle force vector with the axis of rotation, and the effective out-lever is the length of the vector which connects the rotational axis with the bite contact point on the mandible blade, all defined in the plane of rotation. Eqn 2 is in widespread use to model the biomechanics of musculoskeletal lever systems, but a major complexity is only implied: the muscle stress, the pennation angle and the mechanical advantage all depend on the mandibular opening angle (Herring and Herring, 1974; Heethoff and Norton, 2009; Goyens et al., 2015; Weihmann et al., 2015a; Püffel et al., 2023). The resulting variation in bite force with opening angle can be substantial: in *A. cephalotes* majors, bite forces at small opening angles are around 5 times larger than those at large opening angles (see Püffel et al., 2023; and Fig. 2). In order to estimate maximum bite forces from bite forces measured at different opening angles, it is thus necessary to determine how muscle stress, pennation angle and mechanical advantage vary with opening angle:

$$|\mathbf{F}_b|(\theta) = \sigma(\theta) A_{phys} \cos[\phi(\theta)] \frac{|\mathbf{L}_{i,eff}(\theta)|}{|\mathbf{L}_{o,eff}|}. \quad (3)$$

The muscle stress depends on opening angle, because contractions at different opening angles involve different fibre lengths, and muscle has a characteristic force–length dependence (Gordon et al., 1966; Josephson, 1975; Otten, 1987). The variation of stress with fibre length can be characterised by an empirical function  $\sigma(\theta) = \sigma_{max} e^{-\beta[1 - L_f(\theta)/L_{opt}]^2}$ , where  $\beta$  is a shape parameter,  $L_f$  is the average muscle fibre length and  $L_{opt}$  is the fibre length at which muscle stress is maximum (Otten, 1987). We recently demonstrated that the functions  $\cos[\phi(\theta)]$ ,  $|\mathbf{L}_{i,eff}(\theta)|$  and  $L_f(\theta)$  can be accurately predicted from first principles, using morphological reference measurements for the muscle volume, average muscle fibre length, pennation angle and the effective mandible levers from a single opening angle (see Püffel et al., 2023, for a detailed derivation; see Supplementary Materials and Methods for exact mathematical expressions). In order to obtain these reference measurements, we analysed 13 tomographic scans of *A. vollenweideri* leaf-cutter ants across the size range (for details, see Püffel et al., 2021).

We assume that all fibres of the closer muscle attach to the tendon-like apodeme via thin filaments (which holds for 98% of fibres in *A. vollenweideri*; Püffel et al., 2021), and define the physiological cross-sectional area as the muscle volume divided by

the fibre length at which the muscle stress is maximum,  $L_{\text{opt}}$  (Püffel et al., 2023). The maximum muscle stress  $\sigma_{\text{max}}=1.16$  MPa and  $\beta=5.34$  were taken from Püffel et al. (2023), where they were determined experimentally for closely related *A. cephalotes* majors. We make the simplifying assumption that these parameters are size independent, and this assumption is supported by the resulting agreement between theoretical prediction and measured bite force (see below).

The mandibular opening angle  $\theta_{\text{opt}}$  at which the muscle stress is maximum,  $L_f(\theta_{\text{opt}})=L_{\text{opt}}$ , was then estimated via a non-linear least squares numerical fitting routine of Eqn 3 in Python (v. 3.9; Van Rossum and Drake, 2009).  $\theta_{\text{opt}}$  may be reasonably expected to vary with body size, as it is sensitive to head capsule geometry, which changes with size in *A. vollenweideri* (see Püffel et al., 2021; N. Imirzian, F.P., F.R. and D.L., unpublished). In order to investigate the size dependence of  $\theta_{\text{opt}}$ , we only fitted bite force measurements from individuals with a body mass that differed by no more than ~25% from that of the individuals for which we obtained morphological data from microcomputed tomography ( $\mu\text{CT}$ ) scans. Each size class bin contained at least eight bite force measurements, except for the largest and smallest ant, which contained two and three bites, respectively.

In order to implement the opening angle correction across worker sizes, we first characterised the size-dependent relationship between bite force and opening angle as outlined above. Next, we generated a database containing the relationship between predicted bite force, normalised with its maximum,  $|\mathbf{F}^*|$ , opening angle and size. We rescaled the measured forces, corrected via Eqn 1,  $|\mathbf{F}_{\text{b},\theta}|$ , to the force expected at an equivalent mandibular opening angle – the angle  $\theta_{\text{max}}$  at which bite forces are maximal –  $|\mathbf{F}_{\text{b,max}}|=|\mathbf{F}_{\text{b},\theta}|/|\mathbf{F}_{\theta}^*|$ , where  $|\mathbf{F}_{\theta}^*|$  represents the fraction of the maximum bite force produced at  $\theta_{\text{max}}$ . The magnitude of this correction thus depends on both the body mass and the mandibular opening angle of the biting ant; the corrected value used for the final analysis is the maximum bite force the animal can transmit at the distal mandibular tooth (see Fig. 1D).

### Data curation and statistical analysis

We pooled bite force data from all three colonies, because the relationship between bite force and body mass was independent of colony both before and after correcting for differences in opening angle [analysis of covariance (ANCOVA) on  $\log_{10}$ -transformed data, before correction:  $F_{2,242}=1.26$ ,  $P=0.28$ ; after correction:  $F_{2,242}=0.85$ ,  $P=0.43$ ]. Out of 248 bite force measurements (see Table S3), three slightly exceeded the range of calibration forces; two were lower and one higher, but all within 15% of the nearest calibration force. These measurements neither appeared to be outliers nor altered the scaling relationship (see Results), and were hence kept for the analysis. Scaling relationships were characterised with ordinary least squares (OLS) and reduced major axis (RMA) regression models on  $\log_{10}$ -transformed data in R (v. 4.1; <http://www.R-project.org/>). For simplicity, we only report the results of the OLS regressions in the text; the RMA regression results are provided in Tables S1 and S2. Scaling coefficients – the slopes of the regression lines – tend to be higher for RMA regressions (see also LaBarbera, 1989); however, the main conclusions of this study are supported by both.

## RESULTS

### Leaf-cutter ant bite forces increase with strong positive allometry

We measured bite forces of *A. vollenweideri* leaf-cutter ants spanning more than one order of magnitude in body mass,  $m$ .

Measured bite forces  $|\mathbf{F}_{\text{b},m}|$  ranged from a minimum of 31 mN to a maximum of 1029 mN, and were proportional to  $m^{0.79}$  [OLS 95% confidence interval (CI): (0.74, 0.85),  $R^2=0.75$ ; see Fig. S1], suggesting positive allometry (i.e. a scaling relationship steeper than predicted by isometry,  $m^{0.67}$ ). After correcting for force orientation, and bite position along the bite plate and mandible blade, respectively, bite forces,  $|\mathbf{F}_{\text{b},\theta}|$ , ranged between 19 and 901 mN (see Fig. 2 and Eqn 1), and were proportional to  $m^{0.85}$  [OLS 95% CI: (0.79, 0.92),  $R^2=0.74$ ], in substantial excess of the scaling coefficient of  $|\mathbf{F}_{\text{b},m}|$  (see Fig. 3B). However, this scaling relationship was still influenced by systematic differences in mandibular opening angle, which, as expected, were systematically smaller for larger animals [analysis of variance (ANOVA) on  $\log_{10}$ -transformed data:  $F_{1,246}=15.24$ ,  $P<0.001$ ].

In order to correct for systematic differences in opening angle, we first assessed the size dependence of the opening angle,  $\theta_{\text{opt}}$ , at which muscle stress is maximum (see Materials and Methods; Püffel et al., 2023). Notably,  $\theta_{\text{opt}}$  decreased significantly with body mass [OLS: slope= $-0.09$ , 95% CI: ( $-0.15$ ,  $-0.04$ ),  $P<0.01$ ,  $R^2=0.56$ ];  $\theta_{\text{opt}}\approx 70$  deg for a 1.5 mg ant, but  $\theta_{\text{opt}}\approx 50$  deg for a 45 mg ant. Next, we calculated the opening angle at which the bite force is maximum,  $\theta_{\text{max}}$ .  $\theta_{\text{max}}$  may differ from  $\theta_{\text{opt}}$  because it is the opening angle at which the product of the mechanical advantage, the pennation angle and the muscle stress is maximal, as opposed to just muscle stress (see Eqn 3; Püffel et al., 2023).  $\theta_{\text{max}}$  decreased significantly with size [OLS: slope= $-0.06$ , 95% CI: ( $-0.10$ ,  $-0.03$ ),  $P<0.01$ ,  $R^2=0.59$ ; represented by the crosses in Fig. 3A]; the bite forces of a 1.5 and 45 mg ant were maximal at around 65 and 50 deg, respectively. Thus, the difference between  $\theta_{\text{max}}$  and  $\theta_{\text{opt}}$  is small, supporting our earlier conclusion that the musculoskeletal bite apparatus of leaf-cutter ants has a morphology which maximises the magnitude of the peak bite force (see Püffel et al., 2023).

Equivalent bite forces at  $\theta_{\text{max}}$  and the most distal bite point scale with an even stronger positive allometry,  $|\mathbf{F}_{\text{b,max}}|\propto m^{0.90}$  [OLS 95% CI: (0.86, 0.95),  $R^2=0.86$ ]. The increase in scaling coefficient is surprising, because larger ants bit at significantly smaller opening angles; the intuitive expectation is thus that the bite forces of small ants were underestimated, and the scaling coefficient overestimated. However, this argument neglects the significant decrease of  $\theta_{\text{max}}$ , which reverts the effect: because  $\theta_{\text{max}}$  decreases more quickly than the opening angle increases, larger ants were measured at less favourable opening angles, and the scaling coefficient was underestimated.

Together, the four corrections result in a significant increase of the scaling coefficient by 0.11, or about 15% (LMM with correction as fixed and sample number as random effect:  $\chi^2_1=118$ ,  $P<0.001$ ), and in an increase of  $R^2$  from 0.75 to 0.86. The difference in scaling coefficient may appear small, but this impression is misleading: the difference in maximum bite force between ants varying in body mass by a factor of 30 is  $30^{0.90}\approx 22$  compared with  $30^{0.79}\approx 15$  – a drop by about 30%. Clearly, a careful analysis of bite force measurements is required in order to draw robust conclusions about scaling relationships.

## DISCUSSION

Leaf-cutter ants are an ecologically and economically important herbivore (Wirth et al., 2003; Costa et al., 2008), foraging on a wide variety of plants with different mechanical properties (Cherrett, 1972; Nichols-Orians and Schultz, 1989). Key to foraging success is the ability of workers to produce bite forces sufficiently large to cut plant tissues (Clissold, 2007). How does this ability vary with



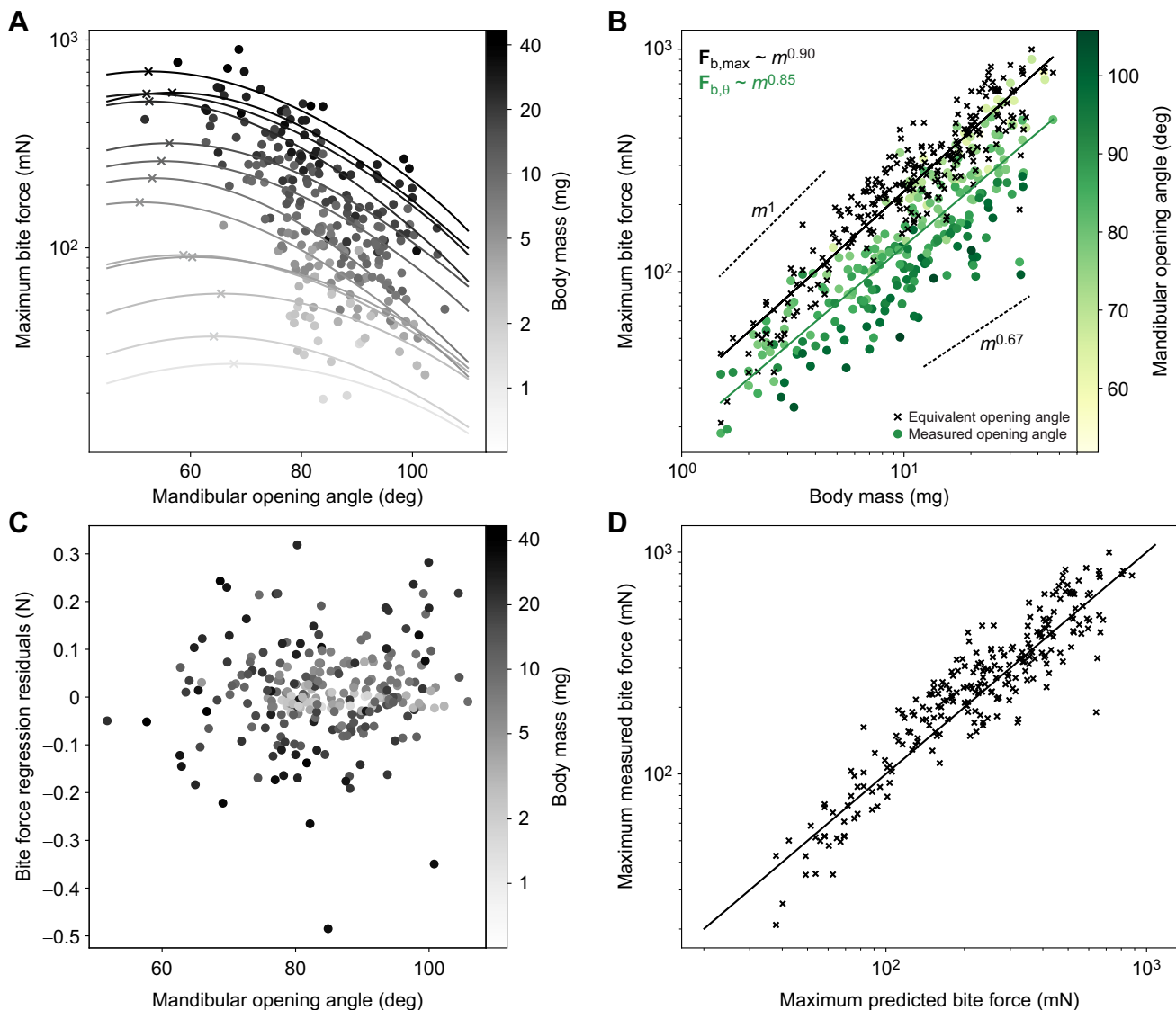


**Fig. 3. Relationship between bite force, mandibular opening angle and body mass.** (A) Bite forces of *A. vollenweideri* workers vary with both mandibular opening angle and body mass. Because ants bite onto two bite plates of finite thickness during bite force measurements (see Fig. 1B,D), bites from smaller ants were measured with larger average opening angles (see also Fig. 2 and Materials and Methods). In order to correct for this systematic difference prior to assessing the scaling of bite force with body mass, the relationship between bite force and opening angle for workers of different body masses was predicted via biomechanical modelling (solid lines; see Eqn 3), and the maximum bite force was extracted for subsequent scaling analyses (crosses; for details on the correction, see Materials and Methods). Note that the maximum bite force occurs at systematically larger opening angles for small workers [ordinary least squares (OLS) regression: slope =  $-0.09$ , 95% confidence interval (CI):  $(-0.15, -0.04)$ ,  $P < 0.01$ ]. (B) Bite forces grew in almost direct proportion to body mass ( $m$ ; upper dashed line), in substantial excess of the prediction from isometry (lower dashed line). The effect of the correction for differences in opening angle is a significant increase of the slope and intercept of the regression line, and of the variation explained by body mass (circles represent uncorrected data; crosses represent opening angle-corrected data). (C) The residuals of the regression of the opening angle-corrected bite forces against mass (black line and crosses in B) are independent of mandibular opening angle (ANOVA:  $F_{1,246} = 2.43$ ,  $P = 0.12$ ), supporting the validity of the biomechanical modelling. (D) Experimentally measured and corrected bite forces are in excellent agreement with theoretical predictions based on biomechanical modelling and regression analysis (bite force  $\sim$  body mass; see crosses in A; Eqn 3), as demonstrated by the identity function (solid line). We note that predicted and corrected forces are not strictly independent; the optimum opening angle, affecting the force prediction, was fitted using the measured bite forces (for further details, see Materials and Methods).

worker size? In order to address this question, we measured the maximum bite forces of *A. vollenweideri* leaf-cutter ants spanning more than one order of magnitude in body mass. In the following discussion, we (i) link the bite force allometry with its morphological and physiological determinants; (ii) discuss the magnitude and scaling of maximum bite forces in the context of foraging ecology; and (iii) place our findings in an evolutionary and comparative context.

### Bite force allometry can be accurately predicted from muscle architecture and head morphology

Maximum bite forces of *A. vollenweideri* workers show strong positive allometry,  $|F_{b,max}| \propto m^{0.90}$ . Because of the large variation in worker size, the effect of this positive allometry is rather extreme: the largest ant workers generate maximum bite forces about 2.5 times higher than a theoretical isometric worker with the same body mass,  $(45/1)^{0.90-0.67} \approx 2.5$ . Can this extreme positive allometry be

understood from the morphology and physiology of the *Atta* bite apparatus?

We have previously extracted the relevant morphological bite force determinants in *A. vollenweideri* workers from tomographic scans (see Püffel et al., 2021). Using these data in conjunction with Eqn 2 led to the prediction that bite forces should scale as  $m^{0.88}$  (95% CI: 0.81, 0.95), a positive allometry largely driven by a disproportionate increase in physiological cross-sectional area of the mandible closer muscle (Püffel et al., 2021). This prediction is in rather close agreement with our bite force measurements. The small difference stems from the fact that we previously extracted the morphological bite force determinants from scans, where the mandibles were maximally closed, whereas  $\theta_{\max}$  varies across sizes (see Fig. 3A). In order to account for this variation in our morphological prediction, and to estimate the intercept of the scaling relationship, we used the stress and force-length shape parameter measured for closely related *A. cephalotes* (Püffel et al., 2023), the change in  $\theta_{\text{opt}}$  as observed in this work, and a biomechanical model which links morphology, opening angle and bite force to directly predict maximum bite forces (see Eqn 3 and Fig. 3A; see also Püffel et al., 2023).

The maximum bite forces predicted by this calculation are proportional to  $m^{0.91}$  [OLS 95% CI: (0.82, 1.01),  $R^2=0.98$ ], with an intercept of 1.42 [units: mN, mg; OLS 95% CI: (1.32, 1.52)]. Both estimates are almost identical to the results obtained from direct measurements:  $m^{0.90}$  (scaling coefficient) [OLS 95% CI: (0.86, 0.95),  $R^2=0.86$ ], 1.46 (intercept) [units: mN, mg; OLS 95% CI: (1.41, 1.51)]. In other words, the ratio between maximum measured and predicted bite forces is close to unity (1.11±0.30), and independent of body mass (ANOVA on  $\log_{10}$ -transformed data:  $F_{1,246}=0.23$ ,  $P=0.63$ ; see Fig. 3D). We thus conclude that the scaling of bite forces can be predicted to reasonable accuracy from morphological measurements.

Predicting bite performance from morphology is of considerable interest to evolutionary biologists, palaeontologists and biomechanists alike, as *in vivo* force measurements are often challenging if not impossible to obtain. Consequently, theoretical models to predict maximum bite force have been developed and deployed for numerous taxa (e.g. Püffel et al., 2023; Erickson et al., 1996; Huber et al., 2006; Heethoff and Norton, 2009; Habegger et al., 2012). In arthropods, the two key obstacles facing such theoretical efforts are the extraordinary variation in reported muscle stresses (e.g. Taylor, 2000; Guschlbauer et al., 2007) and the uncertainty in estimates of the physiological cross-sectional area, which requires knowledge of the optimal fibre length (Püffel et al., 2023). The fact that we were able to accurately predict both the magnitude and scaling of bite forces in *A. vollenweideri* using physiological parameters measured in closely related *A. cephalotes* suggests that muscle stress and shape parameter  $\beta$  are conserved across sizes and within *Atta*; this finding cautiously indicates that the intraspecific and intrageneric variation of bite forces may be predictable based on morphological data alone.

### Positive allometry of bite force has substantial benefits at the colony level

Bite force is a non-pareil performance measure which influences access to food sources and high-quality mating partners (Anderson et al., 2008). As a result, the variation in morphology and physiology of the bite apparatus across species often reflects species-specific needs (Dumont and Herrel, 2003; Gidmark et al., 2013; Goyens et al., 2014; Santana, 2016; Kaczmarek and Gidmark, 2020). What needs have shaped the evolution of bite performance in *Atta*?

*Atta* ants are known for their ‘catholicity of taste’ (Cherrett, 1968; Rockwood, 1976); a single colony may forage on more than 100 plant species at once, spanning a large range of chemical and mechanical properties (Cherrett, 1972; Shepherd, 1985). Foraging is not completely indiscriminate, however: for example, foragers seem to prefer young (tender) over old (tough) leaves from the same plant (Cherrett, 1972; Waller, 1982; Shepherd, 1985; Nichols-Orians and Schultz, 1990). Notably, this preference disappears when pre-cut leaf fragments are offered instead (Nichols-Orians and Schultz, 1989, 1990), suggesting that foraging decisions are not solely driven by plant chemistry but also by mechanical considerations. Because larger ants typically cut tougher and denser leaves than smaller ants (Cherrett, 1972; Wilson, 1980a,b; Nichols-Orians and Schultz, 1989; Wetterer, 1994a,b), we surmise that these mechanical considerations are further confounded by size. From these simple observations emerge two key demands on bite forces in *Atta*: its magnitude must be large enough to cut a representative leaf, and its scaling determines the range of plant leaves that can be cut by workers of different size.

In order to contextualise the magnitude of the bite force, we estimated the forces required to cut leaves. Consider a blade-like tool which exerts a force of magnitude  $F$  to make a cut of length  $dx$  through a thin sheet of thickness  $t$ . The work done,  $\int F dx$ , supplies the energy required to create the new surface arising from the cut,  $G t dx$ , where  $G$  is the energy associated with a unit area of surface; the cutting force then follows as  $F_c \approx G t$ . This calculation provides a lower bound on the required force, because it neglects the influence of friction, tool geometry and sheet bending (e.g. Kamyab et al., 1998; Williams and Patel, 2016; Zhang et al., 2019). Onoda et al. used cutting tests to quantify a proxy for  $G$ , the work per unit fracture length to cut leaf lamina of known thickness, for about 1000 tropical plant species (Onoda et al., 2011; also see Darvell et al., 1996); we note that although *A. vollenweideri* is often referred to as a grass-cutting ant, workers also cut dicotyledonous leaves (Fowler et al., 1986). On the basis of the simple mechanical model and these extensive experimental results, we estimate that the forces required to cut tropical leaves vary between 7 and 828 mN. The median required cutting force of 82 mN can be generated by a worker of about 3 mg (see Fig. 4B), and we submit that this finding strongly suggests that the remarkable magnitude of bite forces in *A. vollenweideri* (see below) arises from the ecological need to cut leaves.

In order to contextualise the positive allometry of bite force, we next calculated the fraction of cuttable leaves as a function of worker size, both for allometric – as experimentally observed ( $|F_{b,\max}| \propto m^{0.90}$ ) – and for hypothetically isometric workers ( $|F_{b,\max}| \propto m^{0.67}$ ; see Fig. 4). A direct comparison between two populations of workers that follow different scaling laws requires us to specify the body mass at which the two scaling lines intersect. Do large workers bite relatively more strongly, or do small workers bite relatively more weakly? This question cannot be answered *a priori*, and we thus refer to three biological arguments instead. First, the worker size distribution in leaf-cutter ant colonies typically has a long right tail, i.e. the vast majority of foraging workers are relatively small (Wilson, 1953, 1980a, 1983b; Wetterer, 1999). Second, large workers are only produced in larger numbers once colonies exceed a critical size (Wilson, 1983b; Wetterer, 1999). Third, larger workers are more ‘costly’ than smaller workers. On the basis of these arguments, increasing the bite force capacity disproportionately may represent a strategy to minimise the cost associated with a unit increase in maximum bite force. A disproportionate decrease of bite forces, in contrast, appears to



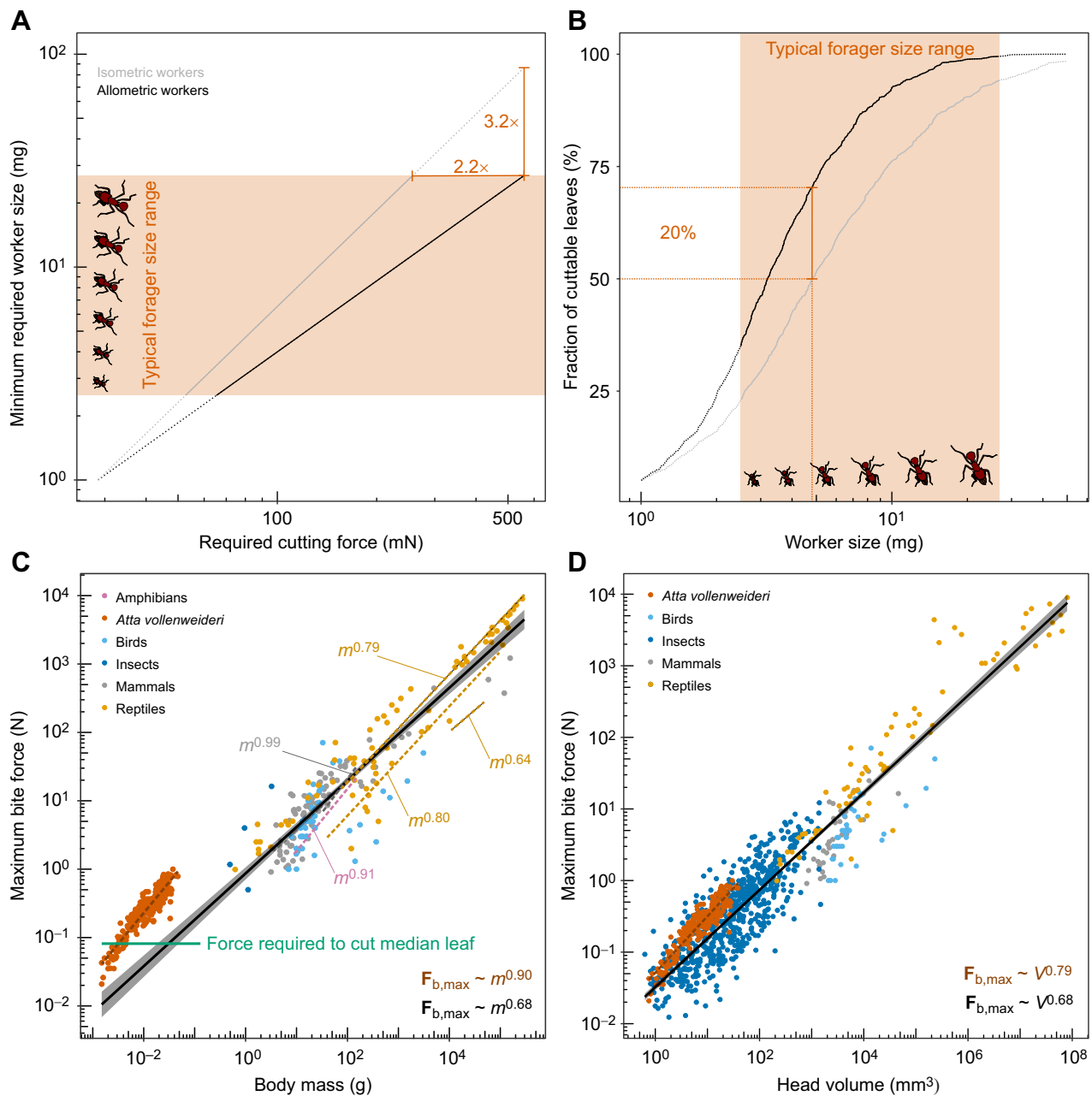


**Fig. 4. Adaptive value of a positively allometric bite force.** (A) We consider possible benefits of the positive allometry of bite force by calculating the minimum worker size that can generate a given force, both for measured positively allometric and hypothetical isometric workers. An isometric worker needs to be about 3 times larger to produce the same bite force as the largest allometric forager; typical *A. vollenweideri* foragers range between 2.5 to 26.9 mg (Röschard and Roces, 2003). (B) An allometric workforce increases the total fraction of cuttable leaves, estimated from measurements on 1000 tropical plant species (Onoda et al., 2011), from around 94% to almost 100%. A medium-sized forager of about 5 mg can cut 70% of leaves; its isometric counterpart can cut only 50%. The positive allometry of bite forces thus probably increases harvesting speed, and provides flexibility in task allocation, so enhancing colony fitness. (C) Positive allometry of bite force ( $F_{b,max}$ ) has been reported in intraspecific studies for several taxa (dashed lines; see Erickson et al., 2003; Becerra et al., 2011; Marshall et al., 2012; Marshall et al., 2014; Lappin et al., 2017; see Table 1). Across distantly related species and a large size range, however, bite forces scale with isometry [black line, mass  $m^{0.68}$ , OLS 95% CI: (0.65, 0.72),  $R^2=0.86$ ]; each circle represents the average maximum bite force for a single species (extracted from Goyens et al., 2014; Weihmann et al., 2015a; Sakamoto et al., 2019). *Atta vollenweideri* ants generate exceptionally large weight-specific bite forces, comparable to those of amniotes 20 times heavier. (D) Relative to their head volume, however, their bite forces are comparable to those of other insects (extracted from Rühr et al., 2022 preprint) and amniotes (Sakamoto et al., 2019), suggesting that leaf-cutter ants have a large weight-specific head volume. Across species, bite forces are isometric [head volume  $V^{0.68}$ , OLS 95% CI: (0.66, 0.70),  $R^2=0.87$ ]. Within *A. vollenweideri*, however, bite force is proportional to  $V^{0.79}$  [OLS 95% CI: (0.75, 0.83),  $R^2=0.86$ ], in excess of isometric predictions, as a result of a disproportionate increase in volume-specific physiological cross-sectional area of the mandible closer muscle (Püffel et al., 2021).

have no obvious biological benefit. Thus, small workers may represent a reasonable generalist ‘starting point’, and we chose a body mass of 1 mg as an intersection mass.

Viewed in this light, the positive allometry of bite force has substantial benefits for the colony for at least two reasons. First, the maximum bite force of an allometric worker with a body mass of

27 mg, at the upper end of forager sizes typically reported in *Atta* (Wetterer, 1990, 1994a,b; Röschard and Roces, 2003; Evison and Ratnieks, 2007), exceeds that of an equally sized isometric worker by a factor of two (see Fig. 4A). Provided that the data reported by Onoda et al. (2011) are representative, this difference increases the fraction of cuttable leaves from 94% to almost 100% (see Fig. 4B). This difference may seem small, but this perception is erroneous: a large isometric forager would need to be 3 times heavier to cut the same fraction of leaves. Second, the smallest worker that can cut the median leaf almost halves in mass between isometric and allometric workers (5 to 3 mg; see Fig. 4B). As the majority of workers are typically small (Wetterer, 1999), the positive allometry thus significantly increases the fraction of the colony that can partake in leaf cutting: an allometric forager of 5 mg can cut up to 70% of leaves, a whopping 20% more than its isometric counterpart. This substantial increase in the size range of ants that can forage on a large number of plant species facilitates flexible task assignment, likely increases harvesting speed and overall influx of nutrients to the nest, and may thus be reasonably expected to enhance colony fitness.

In addition to the positive allometry of maximum bite force, our results revealed a significant decrease in the opening angle at which fibres take their optimum length,  $\theta_{\text{opt}}$ . We note that the last correction step, which led to this conclusion, is complex. In contrast to the first three correction steps, which are based on geometrical relationships and thus have high predictive accuracy, it involves assumptions on muscle physiology, and neglects passive force-length effects due to muscle or connective tissue elasticity (Püffel et al., 2023). In support of the validity of our opening angle correction and the resulting conclusion, three independent lines of evidence may be offered. First, the fully corrected regression analysis explains a substantially larger share of the variation of bite force with mass (86% versus 74% for  $|F_{b,\theta}|$ ; see Fig. 3B). Second, the regression residuals are independent of opening angle [ANOVA:  $F_{1,246}=2.43$ ,  $P=0.12$ ; see Fig. 3C], which does not hold without opening angle correction [ANOVA:  $F_{1,246}=148$ ,  $P<0.001$ ]. Third, the relationship between  $\theta_{\text{opt}}$  and body mass remains significant even after removing the smallest and largest size classes, which contain fewer data points (see Materials and Methods), and are thus associated with higher uncertainty [OLS: slope= $-0.08$ , 95% CI:  $(-0.15, -0.01)$ ,  $P<0.05$ ,  $R^2=0.44$ ]. Our result therefore appears statistically robust, and we next offer a cautious functional interpretation. Ant workers large or small may often forage on the same plant leaf. Although their size differs, the characteristic dimension of the leaf lamina – its thickness – is the same. Because cuts are typically initiated at the leaf edge by drawing the mandibles together like scissors, ants need to produce sufficiently large bite force at a gape width comparable to the leaf lamina thickness. For an ant of 3 mg, the strongest bites occur at a mandible gape of 0.1 mm, approximately half the median leaf thickness (Onoda et al., 2011). At 0.2 mm gape, the opening angle is only a few degrees larger and the force is almost identical ( $\sim 99\%$ ). If, however, this small ant had the same  $\theta_{\text{max}}$  as the largest colony workers, the force at 0.2 mm would be 10% less. We thus suggest that shifts in the optimal length such that the maximum bite force occurs at larger opening angles in small workers may represent an adaptive strategy to counter size-specific disadvantages when workers of different size forage on leaves with a similar thickness.

### Positive allometry of bite force is common within but rare across species

We have discussed the mechanistic origin and ecological significance of the positive allometry of bite forces in *A. vollenweideri*. As a last

step, we aimed to place our findings in a broader comparative and evolutionary context.

To this end, we compared both the scaling and magnitude of bite forces with two extensive datasets including close to 900 species, covering eight orders of magnitude in body mass and head volume (Sakamoto et al., 2019; Rühr et al., 2022 preprint). Regression analysis on  $\log_{10}$ -transformed bite force data for 203 amniote and four insect species against body mass  $m$  (Goyens et al., 2014; Lailvaux et al., 2011; Kelly, 2014; Weihmann et al., 2015a; Sakamoto et al., 2019), and for 139 amniote and 653 insect species against head volume  $V$  (Sakamoto et al., 2019; Rühr et al., 2022 preprint) suggests isometry of bite forces [ $m^{0.68}$ , OLS 95% CI:  $(0.64, 0.72)$ ,  $R^2=0.86$ ;  $V^{0.68}$ , OLS 95% CI:  $(0.66, 0.70)$ ,  $R^2=0.87$ ; see Fig. 4]. The intercepts of the regression, which reflect mass- and head volume-specific bite forces (with mass in g, volume in  $\text{mm}^3$  and force in N), in turn are  $-0.06$  [mass across species: OLS 95% CI:  $(-0.15, 0.03)$ ],  $1.17$  [mass within *A. vollenweideri*: OLS 95% CI:  $(1.07, 1.26)$ ; see Fig. 4C],  $-1.49$  [volume across species: OLS 95% CI:  $(-1.53, -1.44)$ ] and  $-1.29$  [volume within *A. vollenweideri*: OLS 95% CI:  $(-1.33, -1.25)$ ]. Leaf-cutter ants thus appear exceptional in at least two aspects: Their bite forces grow with strong positive allometry, and their weight-specific bite forces are in substantial excess of those for the average amniote and insect, respectively (see also Püffel et al., 2023); the largest ants produce maximum bite forces comparable to those of amniote species at least 20 times heavier (see Fig. 4C), and we have argued above that such a remarkable magnitude of bite forces probably arises from the ecological need to cut tough plant matter. Notably, both the magnitude and the scaling of the bite force of leaf-cutter ants are less remarkable relative to head volume [ $V^{0.79}$ , OLS 95% CI:  $(0.75, 0.83)$ ,  $R^2=0.86$ ; see Fig. 4D]. This discrepancy reflects the fact that a large share of the positive allometry of bite forces in leaf-cutter ants is achieved by a positive allometry of head volume (see Püffel et al., 2021), and that leaf-cutter ants, and perhaps insects in general, have relatively larger heads than vertebrates; indeed, the weight-specific head volume for *A. vollenweideri* is  $671 \pm 74 \text{ mm}^3 \text{ g}^{-1}$  compared with  $209 \pm 134 \text{ mm}^3 \text{ g}^{-1}$  for amniotes (see Fig. 4; Sakamoto et al., 2019).

In the above argument, we have conflated evolutionary allometry involving different species with static allometry involving individuals of the same species at identical ontogenetic stage (Pélabon et al., 2013). In order to analyse whether the static positive allometry of bite forces in leaf-cutter ants is indeed exceptional, and to facilitate a more appropriate comparison of the magnitude of bite forces, we collated results from 22 intraspecific and intrageneric scaling studies on bite force across 12 taxonomic groups (including this study, see Table 1). We note that the majority of intraspecific scaling studies report ontogenetic instead of static scaling coefficients. For each study, we then calculated a  $\log_{10}$ -transformed ‘bite force quotient’,  $\log_{10}\text{BFQ}=\log_{10}(\text{bite force/body mass}^{2/3})$  in  $\text{N/kg}^{2/3}$  (Heethoff and Norton, 2009; van der Meijden et al., 2012) as a measure for weight-specific bite performance. Leaf-cutter ants have the highest  $\log_{10}\text{BFQ}$  apart from coconut crabs, for which bite force was measured at a favourable mechanical advantage (Oka Si et al., 2016); in contrast, we report bite forces for the maximum out-lever and thus small mechanical advantage.

We conclude that leaf-cutter ants are highly specialised to produce large bite forces: (i) they have large heads relative to their body mass compared with vertebrates; (ii) the volume occupancy of mandible closer muscle in these heads and (iii) the geometry of the bite apparatus are close to putative theoretical optima (Püffel et al., 2021, 2023); and (iv) the estimated maximum stress of the mandible

**Table 1. Scaling of maximum bite forces for intraspecific (or intrageneric) studies across various taxa**

Taxon	Statistical model	Scaling	Allometry	log <sub>10</sub> BFQ	Source
Ants	OLS	$m^{0.90}$	p	2.50–2.85	This study
Ants	RMA	$m^{0.97}$	p	2.44–2.90	This study
Birds <sup>‡</sup>	RMA	$m^{0.76-0.88}$	i	0.62–1.22*	Sustaita and Hertel, 2010
Crabs	Not specified	$m^{0.82}$	p	2.66–2.94 <sup>§</sup>	Oka Si et al., 2016
Crabs <sup>‡</sup>	OLS	ML <sup>1.49</sup>	n	No mass reported	Palmer et al., 1999
Crocodylians	OLS	$m^{0.79}$	p	1.92–2.36 <sup>§</sup>	Erickson et al., 2003
Crocodylians	RMA	$m^{0.77-0.78}$	p	1.98–2.40 <sup>§</sup>	Erickson et al., 2014
Frogs	RMA	$m^{0.91}$	p	1.59–1.88	Lappin et al., 2017
Eels	Not specified	BL <sup>2.79-2.94</sup>	p	No mass reported <sup>§</sup>	De Meyer et al., 2018
Lizards <sup>‡</sup>	RMA	SVL <sup>3.83-4.60</sup>	p	1.27–2.34* <sup>§</sup>	Meyers et al., 2002
Lizards	RMA	SVL <sup>2.65-3.37</sup>	p	2.10–2.67* <sup>§</sup>	Herrel and O'Reilly, 2006
Lizards	OLS	$m^{0.57-0.73}$	n, p	2.02–2.36*	Jones et al., 2020
Piranhas	OLS	BL <sup>2.30</sup>	p	2.37–2.47*	Grubich et al., 2012
Ratfish	OLS	BL <sup>2.34</sup>	i	2.07*	Huber et al., 2008
Rodents	RMA	$m^{0.89-0.99}$	p	1.83–2.04	Becerra et al., 2011
Rodents	RMA	$m^{1.11}$	p	1.91–2.06*	Becerra et al., 2013
Rodents	Non-linear RMA	$m^{0.93-1.01}$	p	1.78–2.07	Vassallo et al., 2016
Rodents	OLS	$m^{0.83}$	p	1.78–2.06*	Ginot et al., 2020
Snakes	OLS	$m^{0.28}$	n	0.71–1.14 <sup>§</sup>	Penning, 2017
Turtles	RMA	CL <sup>1.73-2.23</sup>	n, i	1.52–2.53* <sup>§</sup>	Herrel and O'Reilly, 2006
Turtles	RMA	$m^{0.98}$	p	1.90–2.48 <sup>§</sup>	Pfaller et al., 2010
Turtles	Non-linear RMA	$m^{0.80}$	p	1.40–1.85	Marshall et al., 2012
Turtles	Non-linear RMA	$m^{0.64}$	i	1.33	Marshall et al., 2014

The statistical models used to characterise the scaling relationships include ordinary least squares (OLS) and reduced major axis (RMA) regressions performed on log<sub>10</sub>-transformed data; in three studies, a non-linear RMA regression on untransformed data was used instead (Marshall et al., 2012, 2014; Vassallo et al., 2016). The relevant morphological variables are body mass ( $m$ ), or one of several characteristic lengths ( $L$ ): manus length (ML), snout vent length (SVL), carapace length (CL) and body length (BL). Where possible, we selected body mass as a key variable to facilitate comparison with this study. A range of scaling coefficients is given when more than one species (or genus, ‡), intraspecific morphotypes or sexual dimorphism was studied. Significant deviations from isometric scaling, 'i' ( $m^{0.67}$ ,  $L^2$ ) are indicated with a 'p' for positive allometry or 'n' for negative allometry. We calculated a log<sub>10</sub>-transformed bite force quotient (BFQ) based on the reported mass range and regression coefficients (see Heethoff and Norton, 2009; van der Meijden et al., 2012). Because the BFQ is based on isometry, studies that reported allometric scaling are characterised by a range of BFQs. Where regression coefficients for body mass were missing, we calculated the range of BFQ based on the reported mass and bite force ranges (\*). Bite forces that were not measured at the most distal tip of the jaws, or for which the bite position was not explicitly reported, are indicated (§); these data are biased and thus need to be compared with care (see Results and Discussion).

closer muscle is among the highest ever measured (Püffel et al., 2023).

In sharp contrast to the magnitude of bite force, the positive static allometry appears to be less remarkable: around 70% of available intraspecific studies reported significant positive allometry of bite forces, if often less pronounced (including one study that also reported negative allometry for other phenotypes of the same species; Jones et al., 2020). Remarkably, and with the notable exception of bats and finches (Aguirre et al., 2002; van der Meij and Bout, 2004; Herrel et al., 2005; Senawi et al., 2015; Sakamoto et al., 2019), bite force studies involving different genera typically report isometric scaling (Huber et al., 2005; Sakamoto et al., 2019; Deeming, 2022; and see meta-analysis above), or even modest negative allometry (Claussen et al., 2008; Huber et al., 2009; Van Daele et al., 2009; Becerra et al., 2011, 2013; Hite et al., 2019). There thus appears to be a systematic difference between ontogenetic, static and evolutionary scaling of bite forces. To visualise this contrasting tendency, we superimposed a small selection of scaling relationships on the overall evolutionary slope (dashed lines in Fig. 4C). The difference between ontogenetic, static and evolutionary allometry of bite forces is reminiscent of 'transpositional allometry' (Meunier, 1959a,b; Gould, 1971), where group means fall onto one regression line, but within-group variation is governed by a different growth law – a result which appears to be common in biomechanical scaling studies (Schmidt-Nielsen and Knut, 1984; Peattie and Full, 2007; Labonte et al., 2016). Positive allometry of bite forces is probably associated with direct ecological advantages, related, for example, to the quantity and quality of accessible food sources (e.g. Erickson et al., 2003;

Herrel and O'Reilly, 2006; this study). However, increased evolutionary rates of adaptive change in bite forces, required to drive departures from isometry, appear to be the exception rather than the norm, at least across amniotes (Sakamoto et al., 2019).

Four factors may contribute to this seeming discrepancy. First, intraspecific and intrageneric studies on bite performance may be biased toward taxa that may reasonably be expected to face strong ecological or behavioural demands on their bite forces, so increasing the probability of departures from isometry (see also Bonduriansky, 2007). Second, strong positive allometry across many decades of mass is challenging if not impossible to achieve without fundamental 're-design' (Gould, 1966); as an illustrative example, a hypothetical leaf-cutter ant with a body mass of 3 g would have a closer muscle with a volume that exceeds that of its head capsule. Third, in particular, 'static' scaling studies may often be limited by comparatively narrow size ranges (e.g. Herrel et al., 2001; Hite et al., 2019), which increases the influence of biological variation and thus decreases the accuracy of the estimated allometric slope. Fourth, few of the available scaling studies accounted for potential size-specific bias in bite force measurements (see Materials and Methods), and may thus report underestimates or overestimates of the allometric slope. Ultimately, the differences between ontogenetic, static and evolutionary allometry of bite forces reflect species-specific needs, coupled with complex developmental, evolutionary and ecological constraints (e.g. Gould, 1966; Smith, 1984; LaBarbera, 1989; Bonduriansky, 2007; Egset et al., 2012; Pélabon et al., 2013, 2014; Voje and Hansen, 2013; Voje et al., 2014; Bolstad et al., 2015). Untangling the influence of these different factors constitutes an exciting avenue



for comparative and evolutionary work across disparate taxa and a large range of body sizes.

### Conclusions and outlook

Bite forces in leaf-cutter ants scale with strong positive allometry, driven by and accurately predicted from morphological and physiological adaptations of the bite apparatus. Our study adds strong quantitative evidence in support of the hypothesis that size polymorphism and the associated variation in shape broaden a colony's access to plant matter (Wilson, 1980a; Waller, 1989; Wetterer, 1999; Clark, 2006; Hölldobler and Wilson, 2010). However, we acknowledge that the exact relationship between worker size, food plants and cutting performance is complex, and is influenced by nest distance (Roces, 1990), mandibular wear (Schofield et al., 2011) and stridulation of the ant gaster, which can reduce force fluctuations during cutting (Tautz et al., 1995; Roces, 2022). To fully integrate the mechanical results of this study with foraging behaviour, direct measurement of cutting forces with differently sized mandibles as well as behavioural assays with materials of varying mechanical properties are needed; both are currently underway in our laboratory. We hope that such work will increase our understanding of the complex interactions between polymorphism, bite force allometry and foraging ecology in leaf-cutter ants.

### Acknowledgements

We thank Peter Rühr and Alexander Blanke for their support on the validation of our bite force set-up, Daniela Römer for her generous support during the time of the experiments, and Yusuke Onoda for sharing the leaf data.

### Competing interests

The authors declare no competing or financial interests.

### Author contributions

Conceptualization: F.P., D.L.; Methodology: F.P., D.L.; Validation: F.P.; Formal analysis: F.P., D.L.; Investigation: F.P., D.L.; Resources: F.R., D.L.; Data curation: F.P.; Writing - original draft: F.P., D.L.; Writing - review & editing: F.P., F.R., D.L.; Visualization: F.P.; Supervision: D.L.; Funding acquisition: D.L.

### Funding

This study is part of a project that has received funding from the European Research Council (ERC) under the European Union's Horizon 2020 research and innovation programme (grant agreement no. 851705), a European Collaborations Grant by Imperial College London (both to D.L.), and a Company of Biologists travel grant to FP. Open Access funding provided by Imperial College London. Deposited in PMC for immediate release.

### Data availability

All relevant data can be found within the article and its supplementary information.

### References

- Aguirre, L. F., Herrel, A., Van Damme, R. and Matthysen, E. (2002). Ecomorphological analysis of trophic niche partitioning in a tropical savannah bat community. *Proc. R. Soc. Lond. B Biol. Sci.* **269**, 1271-1278. doi:10.1098/rspb.2002.2011
- Anderson, R. A., McBrayer, L. D. and Herrel, A. (2008). Bite force in vertebrates: opportunities and caveats for use of a nonpareil whole-animal performance measure. *Biol. J. Linn. Soc.* **93**, 709-720. doi:10.1111/j.1095-8312.2007.00905.x
- Becerra, F., Echeverría, A., Vassallo, A. I. and Casinos, A. (2011). Bite force and jaw biomechanics in the subterranean rodent talas tuco-tuco (*Ctenomys talarum*) (Caviomorpha: Octodontidae). *Can. J. Zool.* **89**, 334-342. doi:10.1139/z11-007
- Becerra, F., Casinos, A. and Vassallo, A. I. (2013). Biting performance and skull biomechanics of a chisel tooth digging rodent (*Ctenomys tuconax*; Caviomorpha; Octodontidae). *J. Exp. Zool. A Ecol. Genet. Physiol.* **319**, 74-85. doi:10.1002/jez.1770
- Bolstad, G. H., Cassara, J. A., Márquez, E., Hansen, T. F., van der Linde, K., Houle, D. and Pélabon, C. (2015). Complex constraints on allometry revealed by artificial selection on the wing of *Drosophila melanogaster*. *Proc. Natl Acad. Sci. USA* **112**, 13284-13289. doi:10.1073/pnas.1505357112
- Bonduriansky, R. (2007). Sexual selection and allometry: a critical reappraisal of the evidence and ideas. *Evolution* **61**, 838-849. doi:10.1111/j.1558-5646.2007.00081.x
- Burd, M. (1995). Variable load size-ant size matching in leaf-cutting ants, *Atta colombica* (Hymenoptera: Formicidae). *J. Insect Behav.* **8**, 715-722. doi:10.1007/BF01997240
- Burd, M. (1996). Foraging performance by *Atta colombica*, a leaf-cutter ant. *Am. Nat.* **148**, 597-612. doi:10.1086/285942
- Burd, M. (2000a). Body size effects on locomotion and load carriage in the highly polymorphic leaf-cutting ants *Atta colombica* and *Atta cephalotes*. *Behav. Ecol.* **11**, 125-131. doi:10.1093/beheco/11.2.125
- Burd, M. (2000b). Foraging behaviour of *Atta cephalotes* (leaf-cutting ants): an examination of two predictions for load selection. *Anim. Behav.* **60**, 781-788. doi:10.1006/anbe.2000.1537
- Burd, M. (2001). Leaf tissue transport as a function of loading ratio in the leaf-cutting ant *Atta cephalotes*. *Ecol. Entomol.* **26**, 551-556. doi:10.1046/j.1365-2311.2001.00334.x
- Burd, M. and Howard, J. J. (2005). Central-place foraging continues beyond the nest entrance: the underground performance of leaf-cutting ants. *Anim. Behav.* **70**, 737-744. doi:10.1016/j.anbehav.2004.12.012
- Cherrett, J. M. (1968). The foraging behaviour of *Atta cephalotes* L. (Hymenoptera, Formicidae). *J. Anim. Ecol.* **37**, 387-403. doi:10.2307/2955
- Cherrett, J. M. (1972). Some factors involved in the selection of vegetable substrate by *Atta cephalotes* (L.) (hymenoptera: Formicidae) in tropical rain forest. *J. Anim. Ecol.* **41**, 647-660. doi:10.2307/3200
- Clark, E. (2006). Dynamic matching of forager size to resources in the continuously polymorphic leaf-cutter ant, *Atta colombica* (hymenoptera, formicidae). *Ecol. Entomol.* **31**, 629-635. doi:10.1111/j.1365-2311.2006.00826.x
- Claussen, D. L., Gerald, G. W., Kotcher, J. E. and Miskell, C. A. (2008). Pinching forces in crayfish and fiddler crabs, and comparisons with the closing forces of other animals. *J. Comp. Physiol. B* **178**, 333-342. doi:10.1007/s00360-007-0226-8
- Clissold, F. (2007). The biomechanics of chewing and plant fracture: mechanisms and implications. *Adv. Insect Physiol.* **34**, 317-372.
- Costa, A. N., Vasconcelos, H. L., Vieira-Neto, E. H. and Bruna, E. M. (2008). Do herbivores exert top-down effects in neotropical savannas? estimates of biomass consumption by leaf-cutter ants. *J. Veg. Sci.* **19**, 849-854. doi:10.3170/2008-8-18461
- Darvell, B., Lee, P., Yuen, T. and Lucas, P. (1996). A portable fracture toughness tester for biological materials. *Meas. Sci. Technol.* **7**, 954. doi:10.1088/0957-0233/7/6/016
- Deeming, D. (2022). Inter-relationships among body mass, body dimensions, jaw musculature and bite force in reptiles. *J. Zool.* **318**, 23-33. doi:10.1111/jzo.12981
- De Meyer, J., Herrel, A., Belpaire, C., Goemans, G., Ide, C., De Kegel, B., Christiaens, J. and Adriaens, D. (2018). Broader head, stronger bite: *In vivo* bite forces in European eel *Anguilla anguilla*. *J. Fish Biol.* **92**, 268-273. doi:10.1111/jfb.13511
- Dumont, E. R. and Herrel, A. (2003). The effects of gape angle and bite point on bite force in bats. *J. Exp. Biol.* **206**, 2117-2123. doi:10.1242/jeb.00375
- Dussutour, A., Deneubourg, J. L., Beshers, S. and Fourcassie, V. (2008). Individual and collective problem-solving in a foraging context in the leaf-cutting ant *Atta colombica*. *Anim. Cogn.* **12**, 21-30. doi:10.1007/s10071-008-0165-0
- Egset, C. K., Hansen, T. F., Le Rouzic, A., Bolstad, G. H., Rosenqvist, G. and Pelabon, C. (2012). Artificial selection on allometry: change in elevation but not slope. *J. Evol. Biol.* **25**, 938-948. doi:10.1111/j.1420-9101.2012.02487.x
- Erickson, G. M., Kirk, S. D. V., Su, J., Levenston, M. E., Caler, W. E. and Carter, D. R. (1996). Bite-force estimation for *Tyrannosaurus rex* from tooth-marked bones. *Nature* **382**, 706-708. doi:10.1038/382706a0
- Erickson, G. M., Lappin, A. K. and Vliet, K. A. (2003). The ontogeny of bite-force performance in american alligator (*Alligator mississippiensis*). *J. Zool.* **260**, 317-327. doi:10.1017/S0952836903003819
- Erickson, G., Gignac, P., Lappin, A., Vliet, K., Brueggen, J. and Webb, G. (2014). A comparative analysis of ontogenetic bite-force scaling among crocodylia. *J. Zool.* **292**, 48-55. doi:10.1111/jzo.12081
- Evison, S. E. and Ratnieks, F. L. (2007). New role for majors in *Atta* leafcutter ants. *Ecol. Entomol.* **32**, 451-454. doi:10.1111/j.1365-2311.2007.00877.x
- Farji-Brener, A. G. (2001). Why are leaf-cutting ants more common in secondary forest than in old-growth tropical forests? an evaluation of the palatable forage hypothesis. *Oikos* **92**, 169-177. doi:10.1034/j.1600-0706.2001.920120.x
- Farji-Brener, A. G. and Sasal, Y. (2003). Is dump material an effective small-scale deterrent to herbivory by leaf-cutting ants? *Ecoscience* **10**, 151-154. doi:10.1080/11956860.2003.11682761
- Fowler, H., Forti, L., Pereira-da Silva, V. and Saes, N. (1986). Economics of grass-cutting ants. In *Fire Ants and Leaf-Cutting Ants*, pp. 18-35. CRC Press.
- Fowler, H. G., Pagani, M. I., Da Silva, O. A., Forti, L. C. and Vasconcelos, D. L. (1989). A pest is a pest is a pest? the dilemma of neotropical leaf-cutting ants keystone taxa of natural ecosystems. *Environ. Manag.* **13**, 671-675.
- Gidmark, N. J., Konow, N., LoPresti, E. and Brainerd, E. L. (2013). Bite force is limited by the force-length relationship of skeletal muscle in black carp, *Mylopharyngodon piceus*. *Biol. Lett.* **9**, 20121181. doi:10.1098/rsbl.2012.1181

- Ginot, S., Hautier, L., Agret, S. and Claude, J.** (2020). Decoupled ontogeny of *in vivo* bite force and mandible morphology reveals effects of weaning and sexual maturation in mice. *Biol. J. Linn. Soc.* **129**, 558–569. doi:10.1093/biolinnean/blz196
- Gordon, A., Huxley, A. F. and Julian, F.** (1966). The variation in isometric tension with sarcomere length in vertebrate muscle fibres. *J. Physiol.* **184**, 170–192. doi:10.1113/jphysiol.1966.sp007909
- Gould, S. J.** (1966). Allometry and size in ontogeny and phylogeny. *Biol. Rev.* **41**, 587–638. doi:10.1111/j.1469-185X.1966.tb01624.x
- Gould, S. J.** (1971). Geometric similarity in allometric growth: a contribution to the problem of scaling in the evolution of size. *Am. Nat.* **105**, 113–136. doi:10.1086/282710
- Goyens, J., Dirckx, J. and Aerts, P.** (2015). Mechanoreceptor distribution in stag beetle jaws corresponds to the material stress in fights. *Arthropod. Struct. Dev.* **44**, 201–208. doi:10.1016/j.asd.2015.03.003
- Goyens, J., Dirckx, J., Dierck, M., Van Hoorebeke, L. and Aerts, P.** (2014). Biomechanical determinants of bite force dimorphism in *Cyclommatus metallifer* stag beetles. *J. Exp. Biol.* **217**, 1065–1071. doi:10.1242/jeb.091744
- Grubich, J. R., Huskey, S., Crofts, S., Orti, G. and Porto, J.** (2012). Mega-bites: extreme jaw forces of living and extinct piranhas (Serrasalminidae). *Sci. Rep.* **2**, 1–9. doi:10.1038/srep01009
- Guschlbauer, C., Scharstein, H. and Büschges, A.** (2007). The extensor tibiae muscle of the stick insect: biomechanical properties of an insect walking leg muscle. *J. Exp. Biol.* **210**, 1092–1108. doi:10.1242/jeb.02729
- Habegger, M. L., Motta, P. J., Huber, D. R. and Dean, M. N.** (2012). Feeding biomechanics and theoretical calculations of bite force in bull sharks (*Carcharhinus leucas*) during ontogeny. *Zoology* **115**, 354–364. doi:10.1016/j.zool.2012.04.007
- Haykin, S.** (2001). *Communication Systems*, 4th edn. John Wiley & Sons, Inc.
- Heethoff, M. and Norton, R. A.** (2009). A new use for synchrotron x-ray microtomography: three-dimensional biomechanical modeling of chelicerate mouthparts and calculation of theoretical bite forces. *Invertebr. Biol.* **128**, 332–339. doi:10.1111/j.1744-7410.2009.00183.x
- Herrel, A. and O'Reilly, J. C.** (2006). Ontogenetic scaling of bite force in lizards and turtles. *Physiol. Biochem. Zool.* **79**, 31–42. doi:10.1086/498193
- Herrel, A., Spithoven, L., Van Damme, R. and De Vree, F.** (1999). Sexual dimorphism of head size in gallotia galloti: testing the niche divergence hypothesis by functional analyses. *Funct. Ecol.* **13**, 289–297. doi:10.1046/j.1365-2435.1999.00305.x
- Herrel, A., Damme, R. V., Vanhooydonck, B. and Vree, F. D.** (2001). The implications of bite performance for diet in two species of lacertid lizards. *Can. J. Zool.* **79**, 662–670. doi:10.1139/z01-031
- Herrel, A., Podos, J., Huber, S. and Hendry, A.** (2005). Evolution of bite force in Darwin's finches: a key role for head width. *J. Evol. Biol.* **18**, 669–675. doi:10.1111/j.1420-9101.2004.00857.x
- Herring, S. W. and Herring, S. E.** (1974). The superficial masseter and gape in mammals. *Am. Nat.* **108**, 561–576. doi:10.1086/282934
- Hite, N. J., Germain, C., Cain, B. W., Sheldon, M., Perala, S. S. N. and Sarko, D. K.** (2019). The better to eat you with: bite force in the naked mole-rat (*Heterocephalus glaber*) is stronger than predicted based on body size. *Front. Integr. Neurosci.* **13**, 70. doi:10.3389/fnint.2019.00070
- Hölldobler, B. and Wilson, E. O.** (2010). *The Leafcutter Ants: Civilization by Instinct*. New York City: W. W. Norton & Company.
- Huber, D. R., Eason, T. G., Hueter, R. E. and Motta, P. J.** (2005). Analysis of the bite force and mechanical design of the feeding mechanism of the durophagous horn shark *Heterodontus francisci*. *J. Exp. Biol.* **208**, 3553–3571. doi:10.1242/jeb.01816
- Huber, D. R., Weggelaar, C. L. and Motta, P. J.** (2006). Scaling of bite force in the blacktip shark *Carcharhinus limbatus*. *Zoology* **109**, 109–119. doi:10.1016/j.zool.2005.12.002
- Huber, D. R., Dean, M. N. and Summers, A. P.** (2008). Hard prey, soft jaws and the ontogeny of feeding mechanics in the spotted ratfish *Hydrolagus coliei*. *J. R. Soc. Interface* **5**, 941–953. doi:10.1098/rsif.2007.1325
- Huber, D. R., Claes, J. M., Mallefet, J. and Herrel, A.** (2009). Is extreme bite performance associated with extreme morphologies in sharks? *Physiol. Biochem. Zool.* **82**, 20–28. doi:10.1086/588177
- Jones, M. E., Pistevo, J. C., Cooper, N., Lappin, A. K., Georges, A., Hutchinson, M. N. and Holleley, C. E.** (2020). Reproductive phenotype predicts adult bite-force performance in sex-reversed dragons (*Pogona vitticeps*). *J. Exp. Zool. A Ecol. Integr. Physiol.* **333**, 252–263. doi:10.1002/jez.2353
- Josephson, R. K.** (1975). Extensive and intensive factors determining the performance of striated muscle. *J. Exp. Zool.* **194**, 135–153. doi:10.1002/jez.1401940109
- Kaczmarek, E. B. and Gidmark, N. J.** (2020). The bite force–gape relationship as an avenue of biomechanical adaptation to trophic niche in two salmonid fishes. *J. Exp. Biol.* **223**, jeb223180. doi:10.1242/jeb.223180
- Kamyab, I., Chakrabati, S. and Williams, J. G.** (1998). Cutting cheese with wire. *J. Mater. Sci.* **33**, 2763–2770. doi:10.1023/A:1017517332112
- Kelly, C. D.** (2014). Effect of an immune challenge on the functional performance of male weaponry. *Behav. Process.* **108**, 197–203. doi:10.1016/j.beproc.2014.11.001
- LaBarbera, M.** (1989). Analyzing body size as a factor in ecology and evolution. *Annu. Rev. Ecol. Syst.* **20**, 97–117.
- Labonte, D., Clemente, C. J., Dittrich, A., Kuo, C. Y., Crosby, A. J., Irschick, D. J. and Federle, W.** (2016). Extreme positive allometry of animal adhesive pads and the size limits of adhesion-based climbing. *Proc. Natl Acad. Sci. USA* **113**, 1297–1302. doi:10.1073/pnas.1519459113
- Lailvaux, S. P., Zajitschek, F., Dessman, J. and Brooks, R.** (2011). Differential aging of bite and jump performance in virgin and mated *Teleogryllus commodus* crickets. *Evolution* **65**, 3138–3147. doi:10.1111/j.1558-5646.2011.01358.x
- Lappin, A. K. and Jones, M. E.** (2014). Reliable quantification of bite-force performance requires use of appropriate biting substrate and standardization of bite out-lever. *J. Exp. Biol.* **217**, 4303–4312. doi:10.1242/jeb.106385
- Lappin, A. K., Wilcox, S. C., Moriarty, D. J., Stoepler, S. A., Evans, S. E. and Jones, M. E.** (2017). Bite force in the horned frog (*Ceratophrys cranwelli*) with implications for extinct giant frogs. *Sci. Rep.* **7**, 11963. doi:10.1038/s41598-017-11968-6
- Marshall, C. D., Guzman, A., Narazaki, T., Sato, K., Kane, E. A. and Sterba-Boatwright, B. D.** (2012). The ontogenetic scaling of bite force and head size in loggerhead sea turtles (*Caretta caretta*): implications for durophagy in neritic, benthic habitats. *J. Exp. Biol.* **215**, 4166–4174. doi:10.1242/jeb.059956
- Marshall, C. D., Wang, J., Rocha-Olivares, A., Godinez-Reyes, C., Fisler, S., Narazaki, T., Sato, K. and Sterba-Boatwright, B. D.** (2014). Scaling of bite performance with head and carapace morphometrics in green turtles (*Chelonia mydas*). *J. Exp. Mar. Biol. Ecol.* **451**, 91–97. doi:10.1016/j.jembe.2013.11.004
- Meunier, K.** (1959a). Die allometrie des vogelflügels. *Zeitschrift für wissenschaftliche Zoologie* **161**, 444–482.
- Meunier, K.** (1959b). Die größenabhängigkeit der körperform bei vögeln. *Zeitschrift für wissenschaftliche Zoologie* **162**, 328–355.
- Meyers, J. J., Herrel, A. and Birch, J.** (2002). Scaling of morphology, bite force and feeding kinematics in an iguanian and a scleroglossan lizard. In *Topics in Functional and Ecological Vertebrate Morphology*, pp. 47–62. Shaker Publishing.
- Moll, K., Roces, F. and Federle, W.** (2010). Foraging grass-cutting ants (*Atta vollenweideri*) maintain stability by balancing their loads with controlled head movements. *J. Comp. Physiol. A* **196**, 471–480. doi:10.1007/s00359-010-0535-3
- Moll, K., Roces, F. and Federle, W.** (2013). How load-carrying ants avoid falling over: mechanical stability during foraging in *Atta vollenweideri* grass-cutting ants. *PLoS One* **8**, e52816.
- Mueller, U. G., Schultz, T. R., Currie, C. R., Adams, R. M. and Malloch, D.** (2001). The origin of the Attine ant-fungus mutualism. *Q Rev. Biol.* **76**, 169–197. doi:10.1086/393867
- Nichols-Orians, C. M. and Schultz, J. C.** (1989). Leaf toughness affects leaf harvesting by the leaf cutter ant, *Atta cephalotes* (L.) (Hymenoptera: Formicidae). *Biotropica* **21**, 80–83. doi:10.2307/2388446
- Nichols-Orians, C. M. and Schultz, J. C.** (1990). Interactions among leaf toughness, chemistry, and harvesting by attine ants. *Ecol. Entomol.* **15**, 311–320. doi:10.1111/j.1365-2311.1990.tb00813.x
- Oka Si, Tomita, T. and Miyamoto, K.** (2016). A mighty claw: pinching force of the coconut crab, the largest terrestrial crustacean. *PLoS One* **11**: e0166108.
- Onoda, Y., Westoby, M., Adler, P. B., Choong, A. M. F., Clissold, F. J., Cornelissen, J. H. C., Díaz, S., Dominy, N. J., Elgart, A., Enrico, L. et al.** (2011). Global patterns of leaf mechanical properties. *Ecol. Lett.* **14**, 301–312. doi:10.1111/j.1461-0248.2010.01582.x
- Otten, E.** (1987). Optimal design of vertebrate and insect sarcomeres. *J. Morphol.* **191**, 49–62. doi:10.1002/jmor.1051910106
- Palmer, A. R., Taylor, G. M., Barton, A.** (1999). Cuticle strength and the size-dependence of safety factors in *Cancer* crab claws. *Biol. Bull.* **196**, 281–294. doi:10.2307/1542953
- Peattie, A. and Full, R.** (2007). Phylogenetic analysis of the scaling of wet and dry biological fibrillar adhesives. *Proc. Natl Acad. Sci. USA* **104**, 18595–18600. doi:10.1073/pnas.0707591104
- Pélabon, C., Bolstad, G. H., Egset, C. K., Cheverud, J. M., Pavlicev, M. and Rosenqvist, G.** (2013). On the relationship between ontogenetic and static allometry. *Am. Nat.* **181**, 195–212. doi:10.1086/668820
- Pélabon, C., Firmat, C., Bolstad, G. H., Voje, K. L., Houle, D., Cassara, J., Rouzic, A. L. and Hansen, T. F.** (2014). Evolution of morphological allometry. *Ann. N. Y. Acad. Sci.* **1320**, 58–75. doi:10.1111/nyas.12470
- Penning, D. A.** (2017). The scaling of bite force and constriction pressure in kingsnakes (*Lampropeltis getula*): proximate determinants and correlated performance. *Integr. Zool.* **12**, 121–131. doi:10.1111/1749-4877.12216
- Pfaller, J., Herrera, N., Gignac, P. and Erickson, G.** (2010). Ontogenetic scaling of cranial morphology and bite-force generation in the loggerhead musk turtle. *J. Zool.* **280**, 280–289. doi:10.1111/j.1469-7998.2009.00660.x
- Pielström, S. and Roces, F.** (2013). Sequential soil transport and its influence on the spatial organisation of collective digging in leaf-cutting ants. *PLoS One* **8**, e57040.
- Püffel, F., Pouget, A., Liu, X., Zuber, M., van de Kamp, T., Roces, F. and Labonte, D.** (2021). Morphological determinants of bite force capacity in insects: a



- biomechanical analysis of polymorphic leaf-cutter ants. *J. R. Soc. Interface* **18**, 20210424. doi:10.1098/rsif.2021.0424
- Püffel, F., Johnston, R. and Labonte, D.** (2023). A biomechanical model for the relation between bite force and mandibular opening angle in arthropods. *R. Soc. Open Sci.* **10**, 221066. doi:10.1098/rsos.221066
- Roces, F.** (1990). Leaf-cutting ants cut fragment sizes in relation to the distance from the nest. *Anim. Behav.* **40**, 1181-1183. doi:10.1016/S0003-3472(05)80185-X
- Roces, F.** (2002). Individual complexity and self-organization in foraging by leaf-cutting ants. *Biol. Bull.* **202**, 306-312. doi:10.2307/1543483
- Roces, F.** (2022). Vibrational communication outside and inside the nest in leaf-cutting ants. In *Biotremology: Physiology, Ecology, and Evolution*, pp. 411-435. Springer.
- Roces, F. and Hölldobler, B.** (1994). Leaf density and a trade-off between load-size selection and recruitment behaviour in the ant *Atta cephalotes*. *Oecologia* **97**, 1-8. doi:10.1007/BF00317902
- Roces, F. and Hölldobler, B.** (1996). Use of stridulation in foraging leaf-cutting ants: mechanical support during cutting or short-range recruitment signal? *Behav. Ecol. Sociobiol.* **39**, 293-299.
- Roces, F. and Lighton, J. R.** (1995). Larger bites of leaf-cutting ants. *Nature* **373**, 392. doi:10.1038/373392a0
- Roces, F. and Núñez, J. A.** (1993). Information about food quality influences load-size selection in recruited leaf-cutting ants. *Anim. Behav.* **45**, 135-143. doi:10.1006/anbe.1993.1012
- Rockwood, L. L.** (1976). Plant selection and foraging patterns in two species of leaf-cutting ants (*Atta*). *Ecology* **57**, 48-61. doi:10.2307/1936397
- Röschard, J. and Roces, F.** (2002). The effect of load length, width and mass on transport rate in the grass-cutting ant *Atta vollenweideri*. *Oecologia* **131**, 319-324. doi:10.1007/s00442-002-0882-z
- Röschard, J. and Roces, F.** (2003). Fragment-size determination and size-matching in the grass-cutting ant *Atta vollenweideri* depend on the distance from the nest. *J. Trop. Ecol.* **19**, 647-653. doi:10.1017/S0266467403006047
- Röschard, J. and Roces, F.** (2011). Sequential load transport in grass-cutting ants (*Atta vollenweideri*): maximization of plant delivery rate or improved information transfer? *Psyche* **2011**, ID 643127.
- Rudolph, S. G. and Loudon, C.** (1986). Load size selection by foraging leaf-cutter ants (*Atta cephalotes*). *Ecol. Entomol.* **11**, 401-410. doi:10.1111/j.1365-2311.1986.tb00319.x
- Rühr, P. T. and Blanke, A.** (2022). forceX and forceR: a mobile setup and r package to measure and analyse a wide range of animal closing forces. *Method. Ecol. Evol.* **13**, 1-11. doi:10.1111/2041-210X.13631
- Rühr, P. T., Edel, C., Frenzel, M. and Blanke, A.** (2022). A bite force database of 654 insect species. *bioRxiv* doi:10.1101/2022.01.21.477193
- Sakamoto, M., Ruta, M. and Venditti, C.** (2019). Extreme and rapid bursts of functional adaptations shape bite force in amniotes. *Proc. R. Soc. B* **286**, 20181932. doi:10.1098/rspb.2018.1932
- Santana, S. E.** (2016). Quantifying the effect of gape and morphology on bite force: biomechanical modelling and *in vivo* measurements in bats. *Funct. Ecol.* **30**, 557-565. doi:10.1111/1365-2435.12522
- Schmidt-Nielsen, K. and Knut, S. N.** (1984). *Scaling: Why is Animal Size So Important?* Cambridge University Press.
- Schofield, R. M., Emmett, K. D., Niedbala, J. C. and Nesson, M.** (2011). Leaf-cutter ants with worn mandibles cut half as fast, spend twice the energy, and tend to carry instead of cut. *Behav. Ecol. Sociobiol.* **65**, 969-982. doi:10.1007/s00265-010-1098-6
- Schofield, R. M., Choi, S., Coon, J. J., Goggans, M. S., Kreisman, T. F., Silver, D. M. and Nesson, M. H.** (2016). Is fracture a bigger problem for smaller animals? force and fracture scaling for a simple model of cutting, puncture and crushing. *Interface Focus* **6**, 20160002. doi:10.1098/rsfs.2016.0002
- Senawi, J., Schmieder, D., Siemers, B. and Kingston, T.** (2015). Beyond size - morphological predictors of bite force in a diverse insectivorous bat assemblage from Malaysia. *Funct. Ecol.* **29**, 1411-1420. doi:10.1111/1365-2435.12447
- Shepherd, J. D.** (1985). Adjusting foraging effort to resources in adjacent colonies of the leaf-cutter ant, *Atta colombica*. *Biotropica* **17**, 245-252. doi:10.2307/2388225
- Smith, R. J.** (1984). Allometric scaling in comparative biology: problems of concept and method. *Am. J. Physiol. Regul. Integr. Comp. Physiol.* **246**, 152-160. doi:10.1152/ajpregu.1984.246.2.R152
- Sustaita, D. and Hertel, F.** (2010). *In vivo* bite and grip forces, morphology and prey-killing behavior of north American accipiters (Accipitridae) and falcons (Falconidae). *J. Exp. Biol.* **213**, 2617-2628. doi:10.1242/jeb.041731
- Tautz, J., Roces, F. and Hölldobler, B.** (1995). Use of a sound-based vibratome by leaf-cutting ants. *Science* **267**, 84. doi:10.1126/science.267.5194.84
- Taylor, G. M.** (2000). Maximum force production: why are crabs so strong? *Proc. R. Soc. Lond. B Biol. Sci.* **267**, 1475-1480. doi:10.1098/rspb.2000.1167
- Van Daele, P., Herrel, A. and Adriaens, D.** (2009). Biting performance in teeth-digging African mole-rats (*Fukomys*, Bathyergidae, Rodentia). *Physiol. Biochem. Zool.* **82**, 40-50. doi:10.1086/594379
- van der Meij, M. and Bout, R.** (2004). Scaling of jaw muscle size and maximal bite force in finches. *J. Exp. Biol.* **207**, 2745-2753. doi:10.1242/jeb.01091
- van der Meijden, A., Langer, F., Boistel, R., Vagovic, P. and Heethoff, M.** (2012). Functional morphology and bite performance of raptorial chelicerae of camel spiders (solifugae). *J. Exp. Biol.* **215**, 3411-3418.
- Van Rossum, G. and Drake, F. L.** (2009). *Python 3 Reference Manual*. Scotts Valley, CA, USA: CreateSpace.
- Vassallo, A. I., Becerra, F., Echeverría, A. I. and Casinos, A.** (2016). Ontogenetic integration between force production and force reception: a case study in *Ctenomys* (Rodentia: Caviomorpha). *Acta Zool.* **97**, 232-240. doi:10.1111/azo.12119
- Voje, K. L. and Hansen, T. F.** (2013). Evolution of static allometries: adaptive change in allometric slopes of eye span in stalk-eyed flies. *Evolution* **67**, 453-467. doi:10.1111/j.1558-5646.2012.01777.x
- Voje, K. L., Hansen, T. F., Egset, C. K., Bolstad, G. H. and Pelabon, C.** (2014). Allometric constraints and the evolution of allometry. *Evolution* **68**, 866-885. doi:10.1111/evo.12312
- Waller, D.** (1982). Leaf-cutting ants and live oak: the role of leaf toughness in seasonal and intraspecific host choice. *Entomol. Exp. Appl.* **32**, 146-150. doi:10.1111/j.1570-7458.1982.tb03195.x
- Waller, D.** (1989). Size-related foraging in the leaf-cutting ant *Atta texana* (Buckley) (Formicidae: Attini). *Funct. Ecol.* **3**, 461-468. doi:10.2307/2389620
- Weihmann, T., Reinhardt, L., Weißing, K., Siebert, T. and Wipfler, B.** (2015a). Fast and powerful: Biomechanics and bite forces of the mandibles in the American cockroach *Periplaneta americana*. *PLoS One* **10**, e0141226.
- Weihmann, T., Kleinteich, T., Gorb, S. N. and Wipfler, B.** (2015b). Functional morphology of the mandibular apparatus in the cockroach *Periplaneta americana* (Blattodea: Blattellidae) – a model species for omnivore insects. *Arthropod Syst. Phylogeny* **73**, 477-488.
- Wetterer, J. K.** (1990). Load-size determination in the leaf-cutter ant, *Atta cephalotes*. *Behav. Ecol.* **1**, 95-101. doi:10.1093/beheco/1.2.95
- Wetterer, J. K.** (1991). Allometry and geometry of leaf-cutting in *Atta cephalotes*. *Behav. Ecol. Sociobiol.* **29**, 347-351. doi:10.1007/BF00165959
- Wetterer, J. K.** (1994a). Forager polymorphism, size-matching, and load delivery in the leaf-cutting ant, *Atta cephalotes*. *Ecol. Entomol.* **19**, 57-64. doi:10.1111/j.1365-2311.1994.tb00390.x
- Wetterer, J. K.** (1994b). Ontogenetic changes in forager polymorphism and foraging ecology in the leaf-cutting ant *Atta cephalotes*. *Oecologia* **98**, 235-238. doi:10.1007/BF00341478
- Wetterer, J. K.** (1995a). Forager polymorphism and foraging ecology in the leaf-cutting ant, *Atta colombica*. *Psyche* **102**, 131-145. doi:10.1155/1995/10717
- Wetterer, J. K.** (1995b). Forager size and ecology of *Acromyrmex coronatus* and other leaf-cutting ants in costa rica. *Oecologia* **104**, 409-415. doi:10.1007/BF00341337
- Wetterer, J. K.** (1999). The ecology and evolution of worker size-distribution in leaf-cutting ants (Hymenoptera: Formicidae). *Sociobiology* **34**, 119-144.
- Williams, J. G. and Patel, Y.** (2016). Fundamentals of cutting. *Interface Focus* **6**, 20150108. doi:10.1098/rsfs.2015.0108
- Wilson, E. O.** (1953). The origin and evolution of polymorphism in ants. *Q. Rev. Biol.* **28**, 136-156. doi:10.1086/399512
- Wilson, E. O.** (1980a). Caste and division of labor in leaf-cutter ants (Hymenoptera: Formicidae: *Atta*): I. the overall pattern in *A. sextens*. *Behav. Ecol. Sociobiol.* **7**, 143-156. doi:10.1007/BF00299520
- Wilson, E. O.** (1980b). Caste and division of labor in leaf-cutter ants (Hymenoptera: Formicidae: *Atta*): II. the ergonomic optimization of leaf cutting. *Behav. Ecol. Sociobiol.* **7**, 157-165. doi:10.1007/BF00299521
- Wilson, E. O.** (1983a). Caste and division of labor in leaf-cutter ants (Hymenoptera: Formicidae: *Atta*): III. ergonomic resiliency in foraging by *A. cephalotes*. *Behav. Ecol. Sociobiol.* **14**, 47-54. doi:10.1007/BF00366655
- Wilson, E. O.** (1983b). Caste and division of labor in leaf-cutter ants (Hymenoptera: Formicidae: *Atta*): IV. colony ontogeny of *A. cephalotes*. *Behav. Ecol. Sociobiol.* **14**, 55-60. doi:10.1007/BF00366656
- Wirth, R., Herz, H., Ryel, R. J., Beyschlag, W. and Hölldobler, B.** (2003). *Herbivory of Leaf-Cutting Ants: A Case Study on Atta colombica in the Tropical Rainforest of Panama*. Springer Science & Business Media.
- Zhang, B., Shiang, C. S., Yang, S. J. and Hutchens, S. B.** (2019). Y-shaped cutting for the systematic characterization of cutting and tearing. *Exp. Mech.* **59**, 517-529. doi:10.1007/s11340-019-00479-2